DNG and SNG Metamaterial Designs and Realizations for Practical Applications

Richard W. Ziolkowski
ziolkowski@ece.arizona.edu

Department of Electrical and Computer Engineering
The University of Arizona

College of Optical Sciences The University of Arizona

XI School on Metamaterials
Distributed European Doctoral School on Metamaterials
Marrakesh, Morocco
May 6, 2008

Metamaterials (MTMs)
Artificial materials that exhibit electromagnetic responses generally not found in nature

Lycurgus Cup, 300AD

Chartres, France, 1400AD

Inclusions
In a host medium can alter its Electromagnetic Properties

Sir Jagadish Chandra Bose, 1893
Artificial Chiral Materials

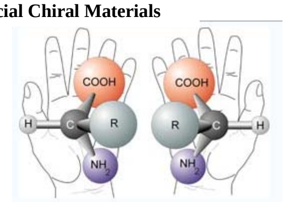

F-117
1983

Metamaterials (MTMs)

Why all the renewed interest in artificial materials??

Cloaking

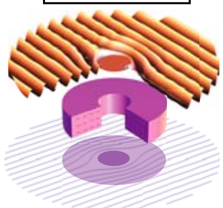

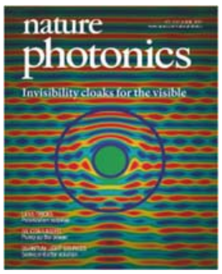

Highly Subwavelength Resonators

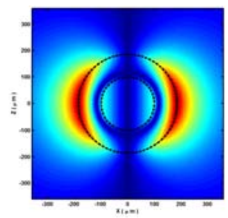

Scattering

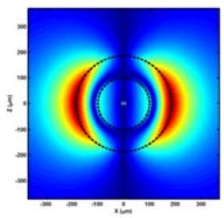

Source

Size ~ $\lambda/100$

Negative ⇨ New Physics and New Engineering Possibilities

The Debye, Lorentz, and Drude linear polarization models produce well-known material responses

Lorentz: Standard 1TD-LM 2TD-LM

$$\partial_t^2 P + \Gamma_e \partial_t P + \omega_0^2 P = \varepsilon_0\, \omega_p^2\, \chi_\alpha E + \varepsilon_0\, \omega_p \chi_\beta\, \partial_t E + \varepsilon_0\, \chi_\gamma\, \partial_t^2 E$$

$$\chi(\omega) = \frac{\omega_p^2\ \chi_\alpha}{-\omega^2 + j\Gamma_e\,\omega + \omega_0^2} + \frac{j\omega_p\ \chi_\beta}{-\omega^2 + j\Gamma_e\,\omega + \omega_0^2} + \frac{-\omega^2\ \chi_\gamma}{-\omega^2 + j\Gamma_e\,\omega + \omega_0^2}$$

Drude:

$$\partial_t^2 P + \Gamma_e\, \partial_t P = \varepsilon_0\, \omega_p^2\, \chi_\alpha E$$

$$\chi(\omega) = \frac{\omega_p^2\ \chi_\alpha}{-\omega^2 + j\Gamma_e\,\omega} = \frac{\omega_p^2\ \chi_\alpha}{-\omega\,(\omega - j\Gamma_e)}$$

Debye:

$$\partial_t P + \Gamma_e P = \varepsilon_0\, \omega_p\, \chi_\alpha E$$

$$\chi(\omega) = \frac{\omega_p\, \chi_\alpha}{j\omega + \Gamma_e}$$

$$\boxed{\chi(\omega) = \frac{\tilde{P}(\omega)}{\varepsilon_0\, \tilde{E}(\omega)}}$$

The Debye, Lorentz, and Drude linear polarization models produce well-known material responses

Lorentz: Standard | 1TD-LM | 2TD-LM

$$\partial_t^2 P + \Gamma_e \partial_t P + \omega_0^2 P = \varepsilon_0 \omega_p^2 \chi_\alpha E + \varepsilon_0 \omega_p \chi_\beta \partial_t E + \varepsilon_0 \chi_\gamma \partial_t^2 E$$

$$\chi(\omega) = \frac{\omega_p^2 \chi_\alpha}{-\omega^2 + j\Gamma_e \omega + \omega_0^2} + \frac{j\omega_p \chi_\beta}{-\omega^2 + j\Gamma_e \omega + \omega_0^2} + \frac{-\omega^2 \chi_\gamma}{-\omega^2 + j\Gamma_e \omega + \omega_0^2}$$

Drude:

$$\partial_t^2 P + \Gamma_e \partial_t P = \varepsilon_0 \omega_p^2 \chi_\alpha E$$

$$\chi(\omega) = \frac{\omega_p^2 \chi_\alpha}{-\omega^2 + j\Gamma_e \omega} = \frac{\omega_p^2 \chi_\alpha}{-\omega(\omega - j\Gamma_e)}$$

Debye:

$$\partial_t P + \Gamma_e P = \varepsilon_0 \omega_p \chi_\alpha E$$

$$\chi(\omega) = \frac{\omega_p \chi_\alpha}{j\omega + \Gamma_e}$$

$$\boxed{\chi(\omega) = \frac{\tilde{P}(\omega)}{\varepsilon_0 \tilde{E}(\omega)}}$$

Where do the negative values appear?

Lorentz real part is negative just above the resonance

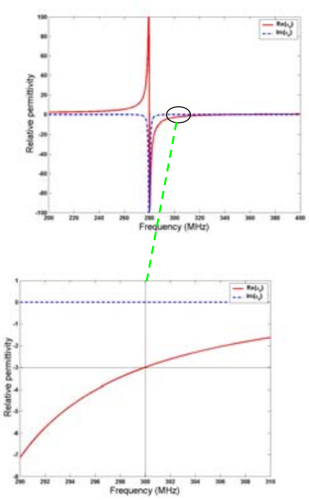

Drude real part is negative for all frequencies below the plasma frequency

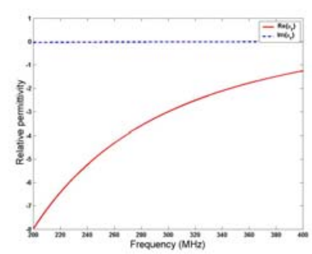

Lorentz behavior = narrow bandwidth
Drude behavior = broad bandwidth

REAL MTMs ARE DISPERSIVE AND LOSSY

ENG versus MNG realizations

	Below 1-10 GHz	Above 1-10 GHz
Easier to achieve	MNG	ENG
Harder to achieve	ENG	MNG

Frequency

1-10 GHz

Metamaterials (MTMs) have exotic properties that may have a high impact on a wide variety of practical applications

ENG ($\varepsilon < 0, \mu > 0$)

DPS ($\varepsilon > 0, \mu > 0$)

μ

UA Unit Cell
Lumped element
~ λ / 100

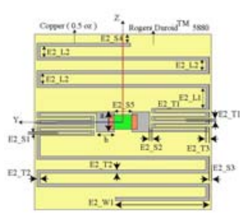

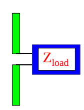

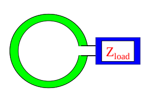

UA
Electric and Magnetic
Molecules
for
RAMs

Zero-index

ε

DNG ($\varepsilon < 0, \mu < 0$)

MNG ($\varepsilon > 0, \mu < 0$)

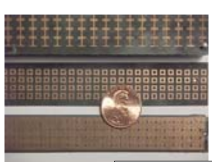

UA Low Loss
DNG and SNG
X-band elements

UA CLL AMC at X-band

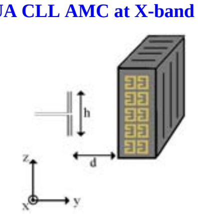

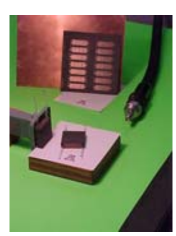

~ -0.3dB/cm

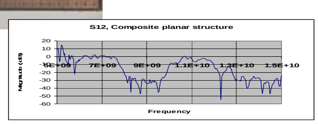

Metamaterials (MTMs) have exotic properties that may have a high impact on a wide variety of practical applications

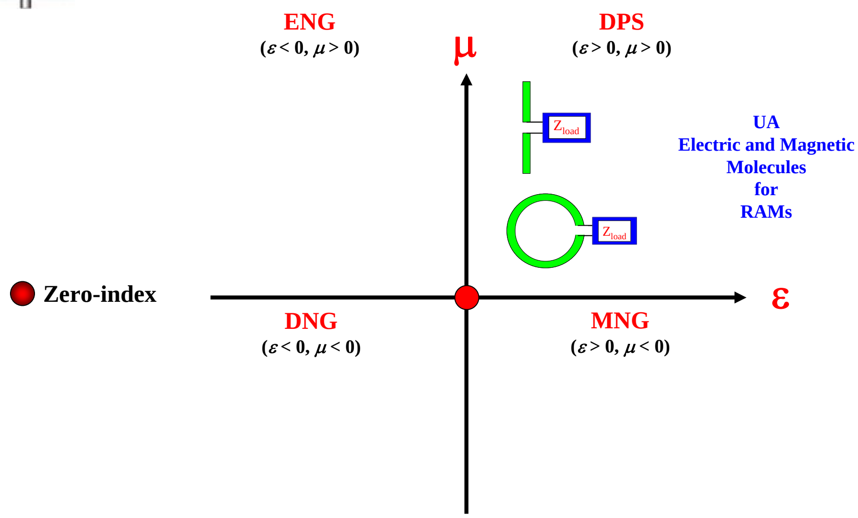

EM Properties of aggregates of atoms / molecules are typically characterized by their electric and magnetic dipole moments

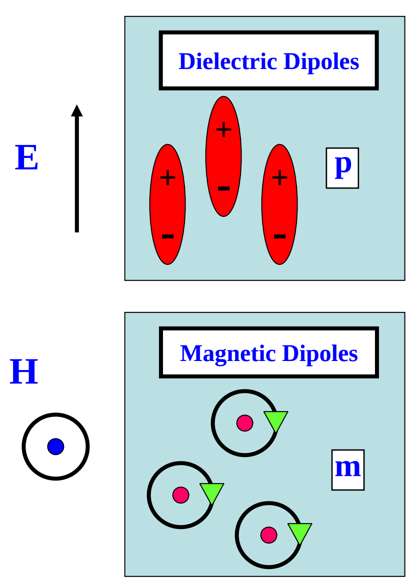

$\mathbf{P} = \Sigma_i \, \mathbf{p}_i / V$

$= \varepsilon_0 \, \chi_e \, \mathbf{E}$

$\varepsilon = \varepsilon_0 \, (1 + \chi_e)$

χ_e = electric susceptibility

$\mathbf{M} = \Sigma_i \, \mathbf{m}_i / V$

$= \chi_m \, \mathbf{H}$

$\mu = \mu_0 \, (1 + \chi_m)$

χ_m = magnetic susceptibility

Artificial electric and magnetic molecules have been designed that produce novel material responses

Electric molecule:
Small Loaded Dipole Antenna

Magnetic molecules:
Small Loaded Loop Antenna

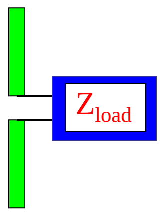

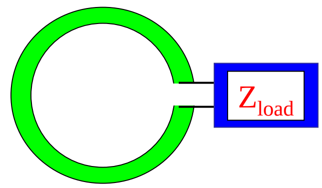

Tailored
Polarization Behavior

Tailored
Magnetization Behavior

F. Auzanneau (CEA-CESTA, France) & R. W. Ziolkowski, 1997-1999

1628 IEEE TRANSACTIONS ON MICROWAVE THEORY AND TECHNIQUES, VOL. 46, NO. 11, NOVEMBER 1998

Microwave Signal Rectification Using Artificial Composite Materials Composed of Diode-Loaded Electrically Small Dipole Antennas

Fabrice Auzanneau and Richard W. Ziolkowski, *Fellow, IEEE*

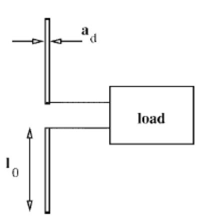

Fig. 1. Basic description of the electrically small loaded dipole antenna.

Model	dipole's load	
Debye	R	
TD Debye	R/C	C/(R-C)
Lorentz	R-L-C	
TD Lorentz	L/R	R-(R/C)
	R-(R/L)	C-(R/L)
	R/(R-C)	
2TD Lorentz	R/L/C	C/(R-L)
	C/(R-L-C)	R/C/(R-L)
	R/C/(R-C)	C-(R/L/C)
TD AZ	L-(R/C)	L-(R/L)
	L/(R-L)	R-L-(R/C)
	R-L-(R/L)	
2TD AZ	R-(L/C)	R/(L-C)
	R-(R/L/C)	R/(R-L-C)
	L/(R-C)	(L-C)/(R-C)
	(R/L)-(R/C)	(R-C)/(R-L)
3TD-AZ	(L/C)-(R/C)	(L/C)-(R/L)
	(R/C)-(R/L/C)	R/C/(L-C)
	R/C/(R-L-C)	
2TD 4^{th} order	L-(R/L/C)	(L-C)/(R-L)
	(L-C)/(R-L-C)	(R-L)/(R-L-C)
	(R-L-C)/(R-L-C)	R-L-(L/C)
	R-L-(R/L/C)	
3TD 4^{th} order	(R/L)-(R/L/C)	(R-C)/(R-L-C)
4TD 4^{th} order	(L/C)-(R/L/C)	(R/L/C)-(R/L/C)
3TD 5^{th} order	L/(R-L-C)	

- $\Longleftrightarrow$ 'in series' — / $\Longleftrightarrow$ 'in parallel'

Several material models had been developed and studied. They produce a variety of novel electromagnetic responses.

Lorentz material

$$\partial_t^2 P + \Gamma_e \partial_t P + \omega_0^2 \; P = \varepsilon_0 \; \omega_p^2 \; \chi_\alpha \, E$$

Time derivative Lorentz material (TDLM)

$$\partial_t^2 P + \Gamma_e \partial_t P + \omega_0^2 \; P = \varepsilon_0 \; \omega_p^2 \; \chi_\alpha \, E + \varepsilon_0 \; \omega_p \; \chi_\beta \, \partial_t \, E$$

Two time derivative Lorentz material (2TDLM)

$$\partial_t^2 P + \Gamma_e \partial_t P + \omega_0^2 \; P = \varepsilon_0 \; \omega_p^2 \; \chi_\alpha \, E + \varepsilon_0 \; \omega_p \; \chi_\beta \, \partial_t \, E + \varepsilon_0 \; \chi_\gamma \, \partial_t^2 \, E$$

These models have been implemented and tested in our 1D, 2D, and 3D FDTD simulators
The 2TDLM model has been used to achieve ABCs for lossy media

The 2TDLM model produces a causal MTM response

$$\partial_t^2 P + \Gamma_e \partial_t P + \omega_0^2 \; P = \varepsilon_0 \; \omega_p^2 \; \chi_\alpha \, E + \varepsilon_0 \; \omega_p \; \chi_\beta \, \partial_t \, E + \varepsilon_0 \; \chi_\gamma \, \partial_t^2 \, E$$

$$\chi(\omega) = \frac{\omega_p^2 \; \chi_\alpha + j\omega\,\omega\,\chi_\beta - \omega^2 \; \chi_\gamma}{-\omega^2 + j\,\Gamma_e\,\omega + \omega_0^2}$$

$$\varepsilon(\omega) = \varepsilon_0 \left[1 + \chi(\omega)\right]$$

This implies controllable low and high frequency limits

$$\lim_{\omega \to 0} \frac{\varepsilon(\omega)}{\varepsilon_0} = 1 + \frac{\omega_p^2}{\omega_0^2} \; \chi_\alpha \qquad\qquad \lim_{\omega \to \infty} \frac{\varepsilon(\omega)}{\varepsilon_0} = 1 + \chi_\gamma$$

DC limit　　　　High freq limit

Uniaxial 2TDLM medium was designed to act as a (Maxwellian) Perfectly Matched Layer for FDTD ABCs

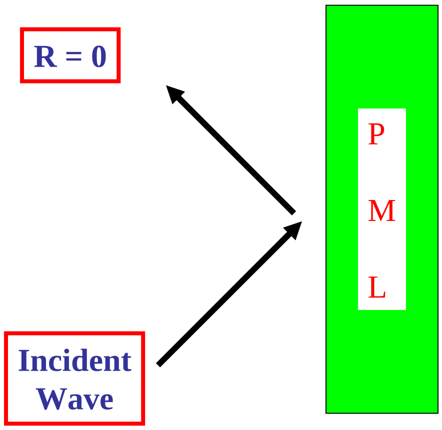

Independent of
- * frequency
- * angle of incidence

ABCs
Stealth
EMI/EMC
PCS
Anechoic Chambers

Electromagnetic absorbers have many useful applications

Considered bi-anisotropic molecules

Journal of Electromagnetic Waves and Applications, Vol. 12, 353–370, 1998

THEORETICAL STUDY OF SYNTHETIC BIANISOTROPIC MATERIALS

F. Auzanneau and R. W. Ziolkowski

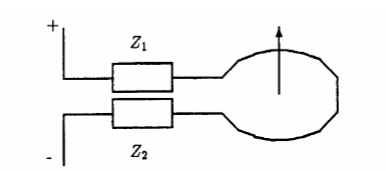

Figure 2. Left bianisotropic molecule.

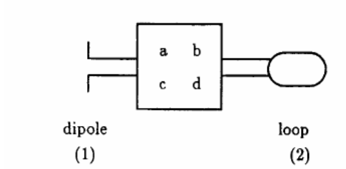

Figure 3. Transmission matrix concept.

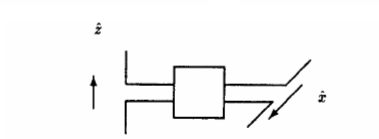

Figure 7. Polarization transforming molecule.

Considered active molecules

1330 IEEE TRANSACTIONS ON ANTENNAS AND PROPAGATION, VOL. 47, NO. 8, AUGUST

Artificial Composite Materials Consisting of Nonlinearly Loaded Electrically Small Antennas: Operational-Amplifier-Based Circuits with Applications to Smart Skins

Fabrice Auzanneau and Richard W. Ziolkowski, *Fellow, IEEE*

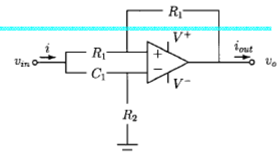

Fig. 11. Phase shifter circuit.

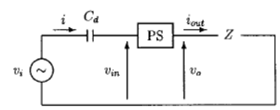

Fig. 12. Phase-shifter circuit in an electric molecule.

Curve Shaper Molecule

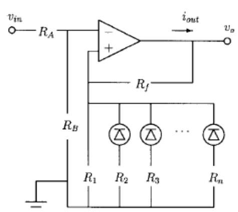

Fig. 14. Curve-shaper circuit. Approximation by n linear segments.

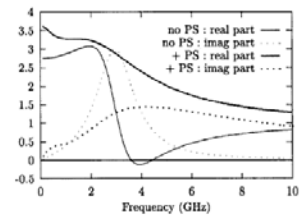

Fig. 13. Phase shifter circuit is inserted into a dielectric Lorentz model Comparison of the relative permittivity ϵ_r with and without the PS circu enhancement.

Volumetric 3D metamaterial realized as a stack of 2D planar metamaterial realizations

Ziolkowski
Bi-Anisotropics Meeting
Ghent, Belgium
2004

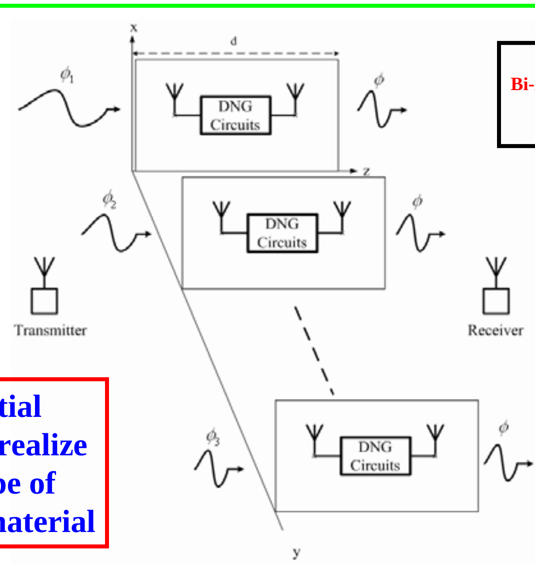

Potential "how to" realize any type of 3D metamaterial

HP-ADS layout of an elementary 2D-3D metamaterial molecule

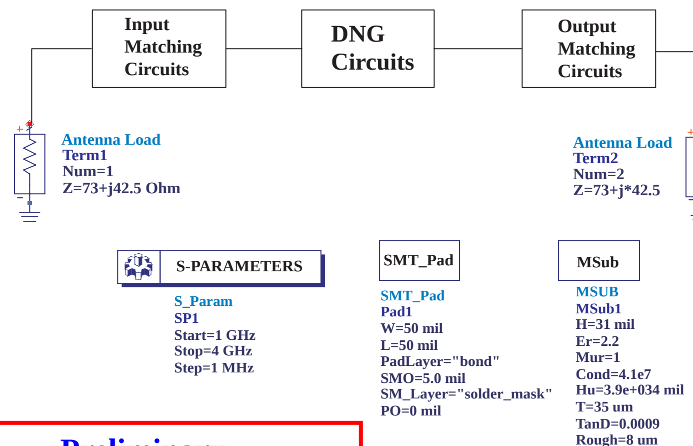

Preliminary results were promising (circa 2004)

Recent considerations

MICROWAVE AND OPTICAL TECHNOLOGY LETTERS / Vol. 31, No. 3, November 5 2001

META-MATERIALS WITH WIDEBAND NEGATIVE PERMITTIVITY AND PERMEABILITY

S. A. Tretyakov[1]

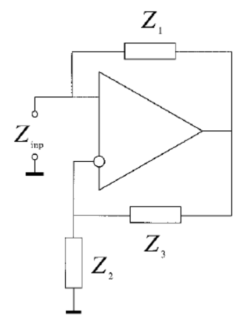

Figure 1 Operational amplifier single-stage impedance inverter

MICROWAVE AND OPTICAL TECHNOLOGY LETTERS / Vol. 49, No. 10, October 2007

AN ARCHITECTURE FOR ACTIVE METAMATERIAL PARTICLES AND EXPERIMENTAL VALIDATION AT RF

Bogdan-Ioan Popa and Steven A. Cummer

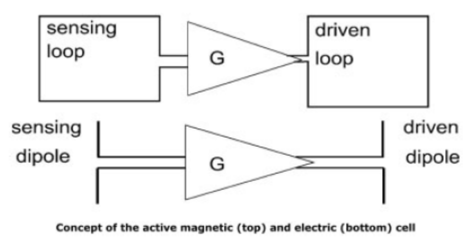

Figure 1 Concept of the active magnetic (top) and electric (bottom) cell

Metamaterials (MTMs) have exotic properties that may have a high impact on a wide variety of practical applications

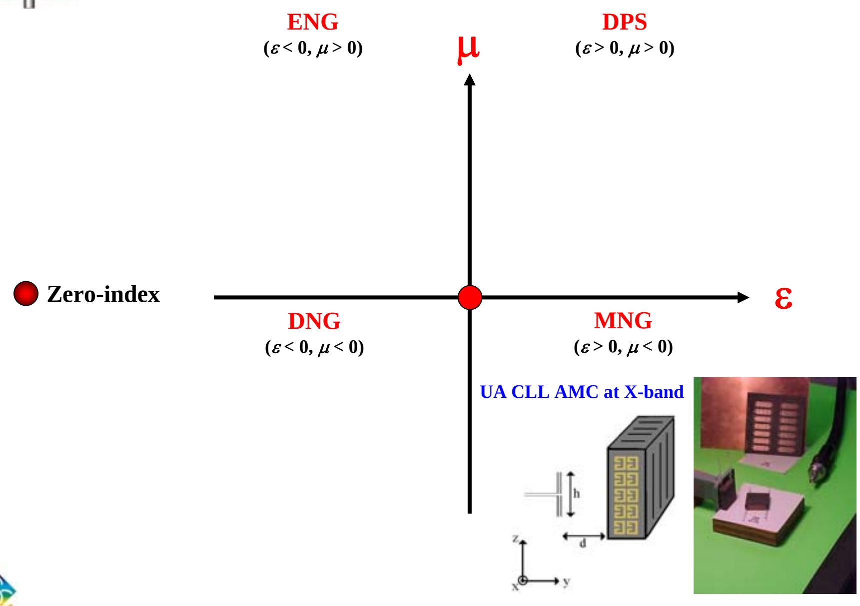

The scattering properties of PEC and PMC slabs are different

Out-of-Phase Reflection

- $E_{tan} = 0$
- $|\Gamma| = +1$
- $\phi_\Gamma = \pi$

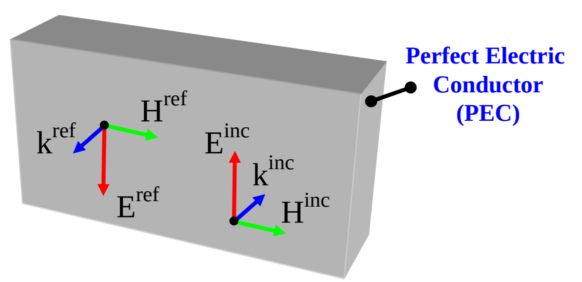

In-Phase Reflection

- $H_{tan} = 0$
- $|\Gamma| = +1$
- $\phi_\Gamma = 0$

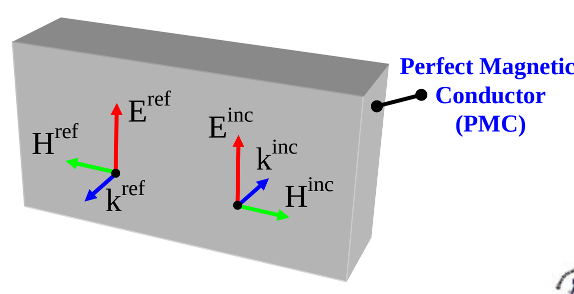

Artificial Magnetic Conductors (AMCs)

- AMCs are high-impedance surfaces often generated by
  - a) incorporating a special texture on host surfaces, or
  - b) artificially fabricated inhomogeneities embedded in host media
- Two important parameters, electrical permittivity ε and magnetic permeability μ, determine the response of the material
- The physical structure of 2-D or 3-D array of inclusions are much smaller than the wavelength

Split Ring Resonators (SRRs) **Capacitively Loaded Loops (CLLs)**

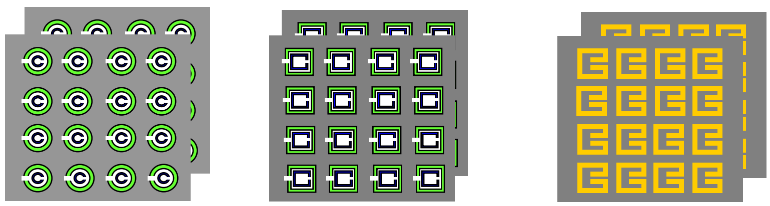

High-Impedance Electromagnetic Surfaces

Mushroom Surface

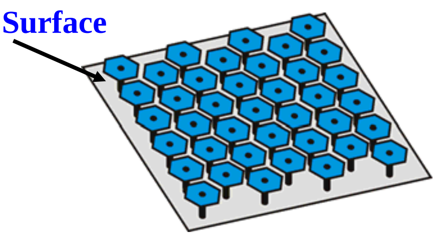

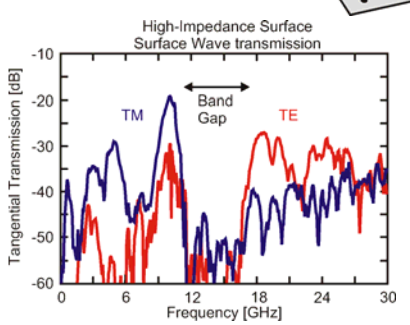

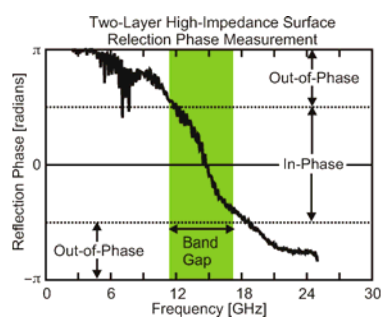

Many Thanks to Dr. Dan Sievenpiper, HRL, for this slide

The reflection and transmission coefficients for the scattering of a normally incident plane wave from a slab are readily derived

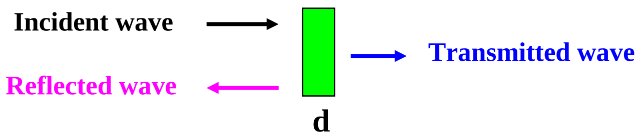

Wave impedance $\eta = \sqrt{\dfrac{\mu}{\varepsilon}}$ $\qquad \eta \to \infty$

Reflection $S_{11} = \dfrac{(\eta-\eta_0)}{(\eta+\eta_0)} \dfrac{1-e^{-j2kd}}{1-(\frac{\eta-\eta_0}{\eta+\eta_0})^2 e^{-j2kd}}$ $\qquad \lim_{\eta\to\infty} S_{11} = 1 \Leftrightarrow$ Independent of d

Transmission $S_{21} = \dfrac{4\eta\eta_0}{(\eta+\eta_0)^2} \dfrac{e^{-j2kd}}{1-(\frac{\eta-\eta_0}{\eta+\eta_0})^2 e^{-j2kd}}$ $\qquad \lim_{\eta\to\infty} S_{21} = 0$

PMC Surface Realization Using UC-PBG

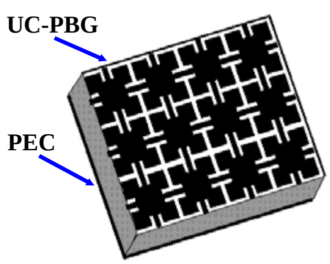

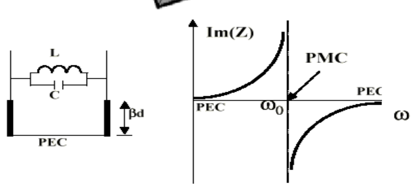

Equivalent Circuit Model

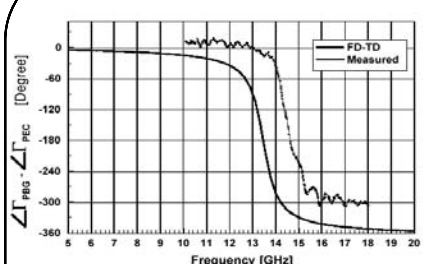

Reflection coefficients measured for PBG structure and PEC surface

- Phase difference = 180^0 @ 14.5 GHz
- Magnitude = 1 at all frequency

Many Thanks to Prof. Tatsuo Itoh, UCLA, for this slide

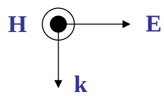

SRR Design with Dimensions

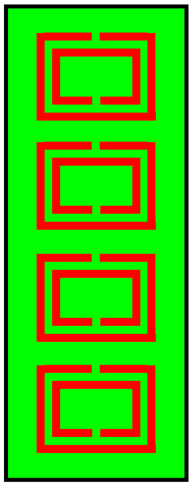

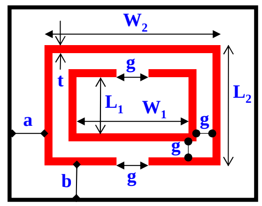

One element unit cell

g	10 mils
t	10 mils
L_1	55 mils
W_1	55 mils
L_2	95 mils
W_2	95 mils
a	25 mils
b	20 mils

100 mils = 2.54 mm

HFSS calculated S_{11} values for the SRR MTM with a depth of 1, 2, 3, 4 SRR elements show complete reflectivity near the design frequency of 10GHz

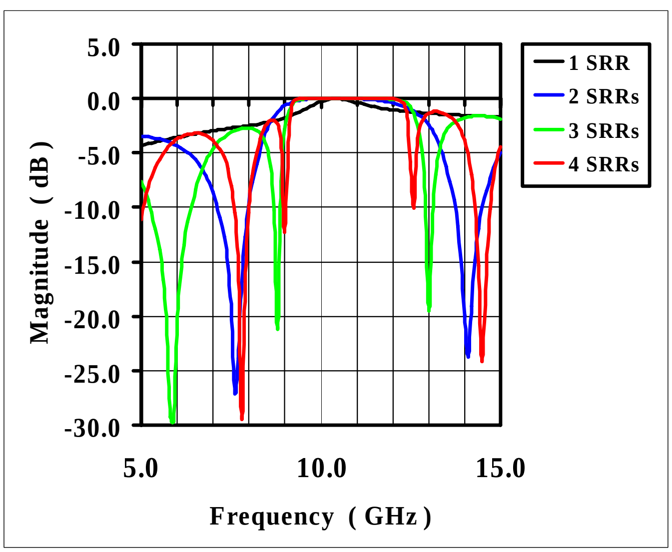

HFSS calculated S_{11} values for the SRR MTM with a depth of 4 SRR elements show that it acts as a PMC near the design frequency of 10GHz

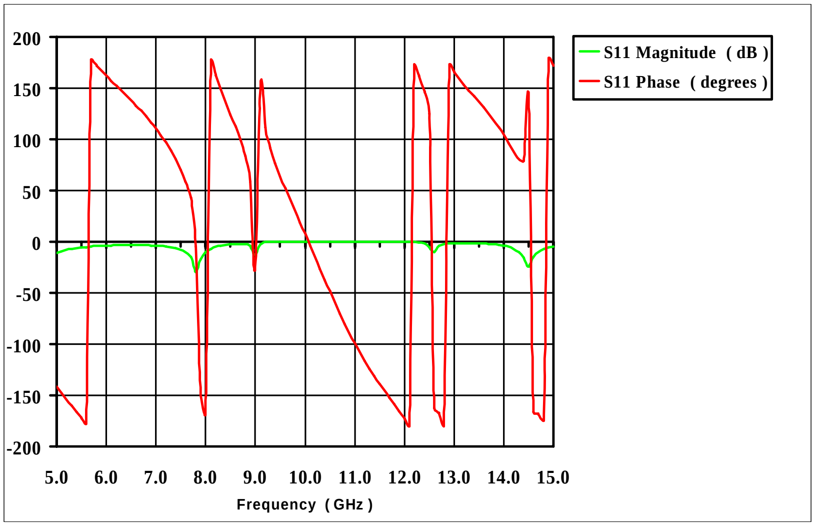

CLL Design with Dimensions

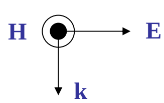

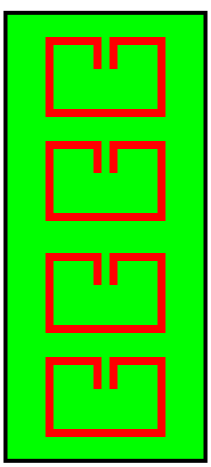

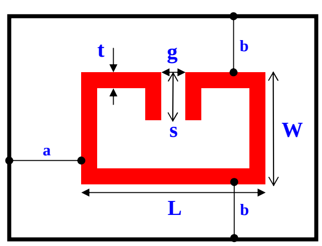

One element unit cell

t	10 mils
G2	10 mils
s	17.2 mils
W	80 mils
L	120 mils
a	40 mils
b	40 mils

100 mils = 2.54 mm

HFSS calculated S_{11} values for the SRR MTM with a depth of 1, 2, 3, 4 CLL elements show complete reflectivity near the design frequency of 10GHz

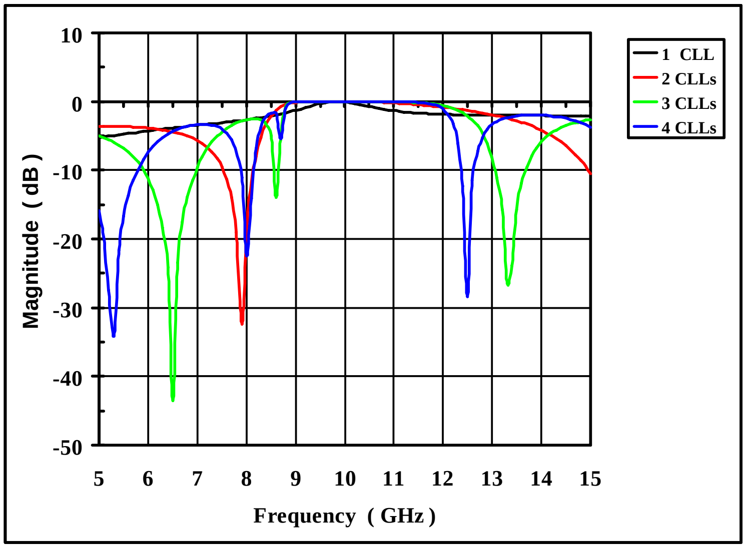

HFSS calculated S_{11} values for the CLL MTM with a depth of 4 CLL elements show that it acts as a PMC near the design frequency of 10GHz

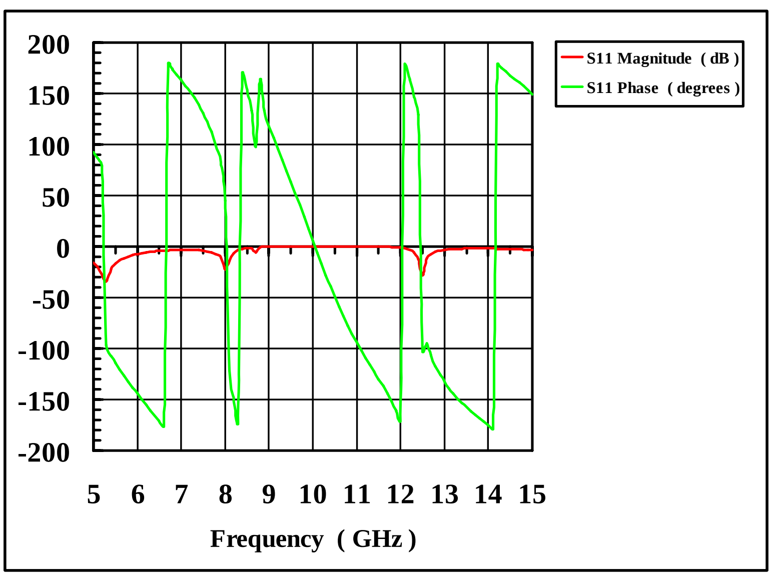

HFSS calculated S_{11} values for the CLL MTM with a depth of 4 CLL elements show that it acts as a PMC near the design frequency of 10GHz

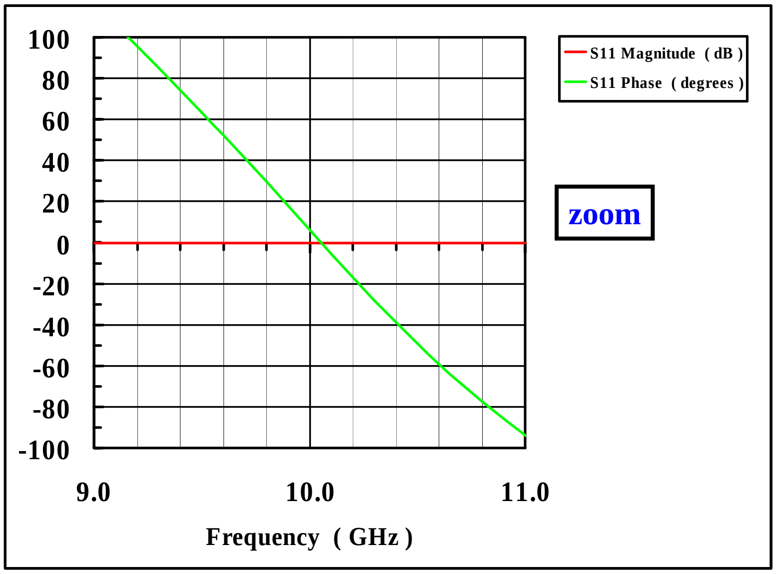

“Final” CLL Metamaterial Structure

- “Precisely cut, aligned” and assembled of 161 strips

The CLL MTM was measured with a free space measurement system

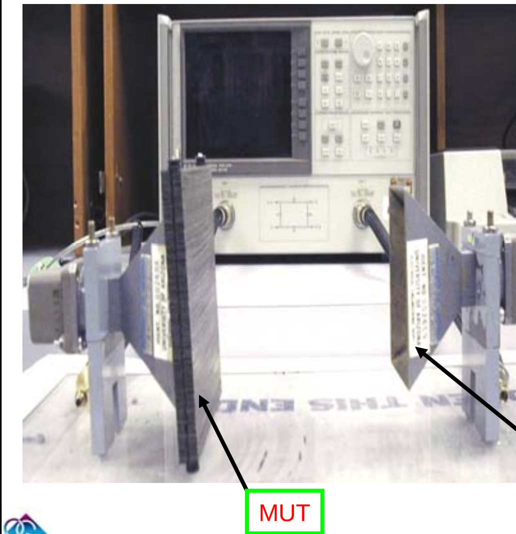

- Measure the CLL MTM with its designed orientation
- Measure the CLL MTM with a 90° rotation
- HP 8720C network analyzer to measure the S-parameters

Measured magnitude of S_{21} for the CLL MTM slab

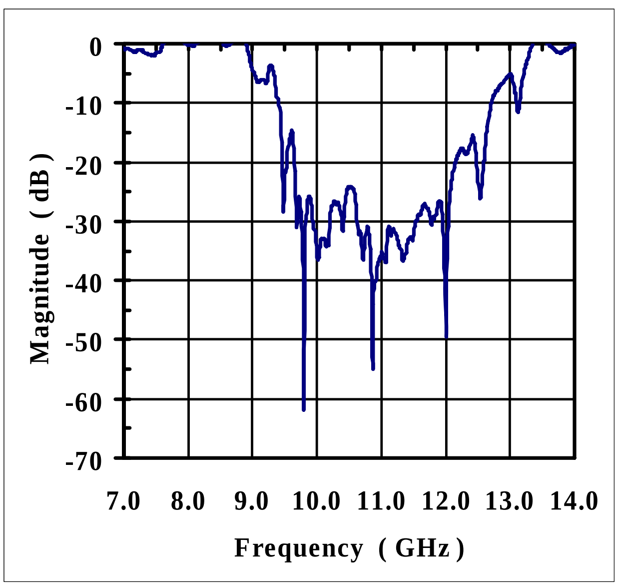

Measured magnitude of S_{11} for the CLL MTM slab

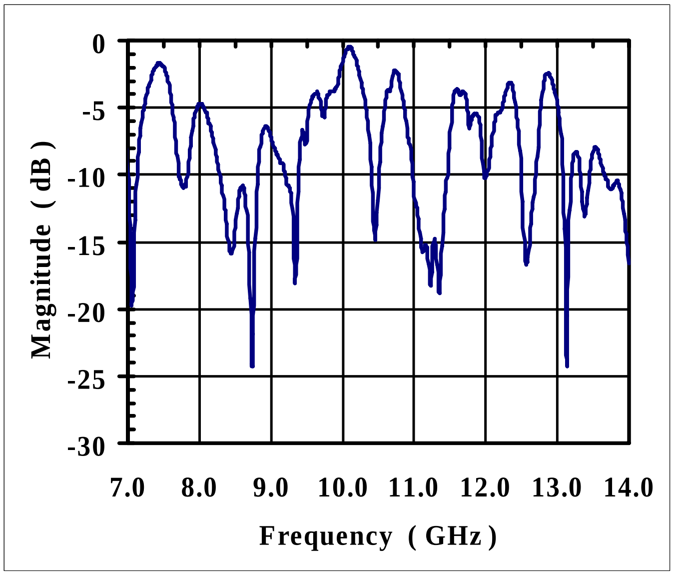

Phase Reference Plane measurement was achieved with a reference copper plate

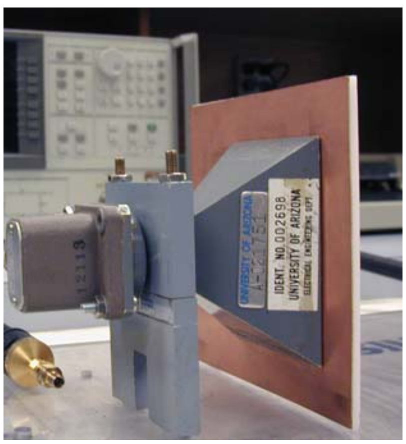

- A copper plate is placed over the mouth of the flange of the transmit antenna

Measured phase of S_{11} for the CLL MTM slab and for the reference plate

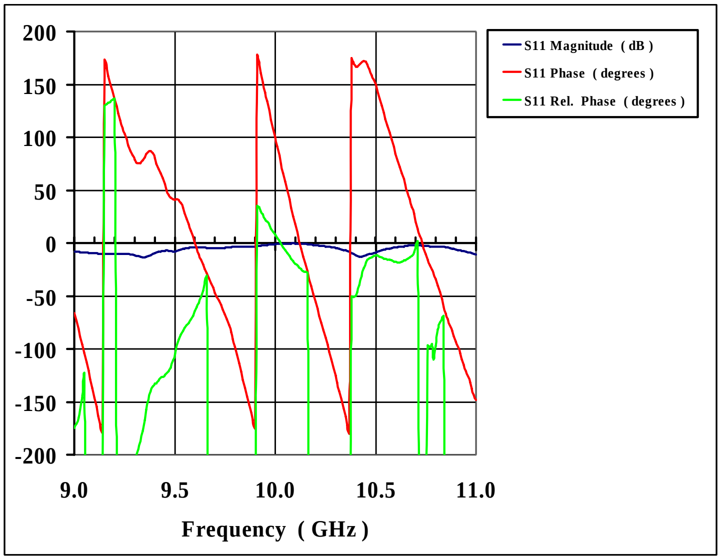

Measured magnitude and phase of S_{11} for the CLL MTM slab verifies the predicted PMC behavior

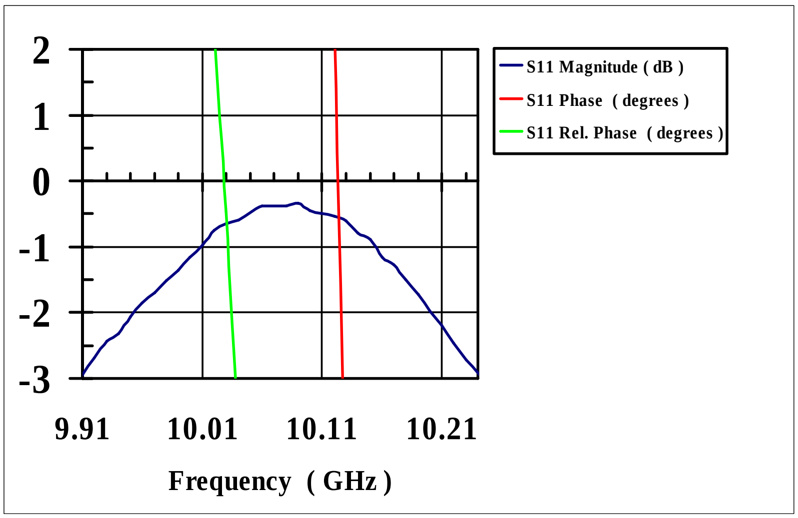

Measured magnitude of S_{11} for the CLL MTM slab in 90^{o} fixed rotatation demonstrates the expected anisotropy

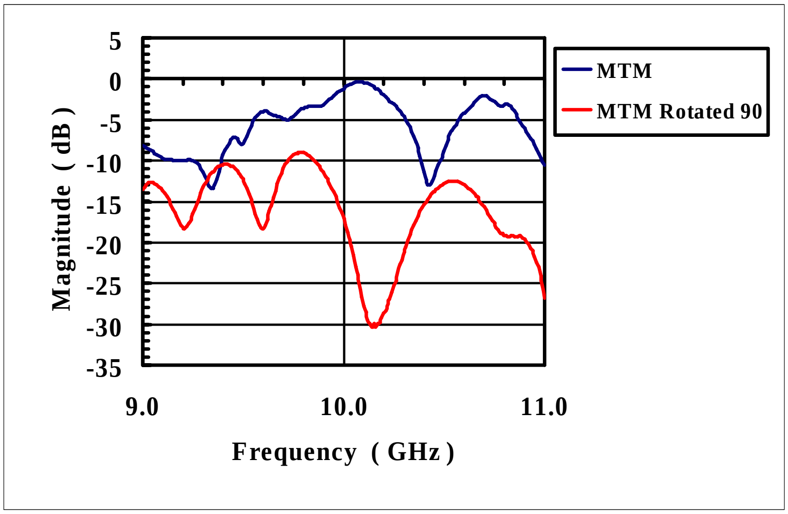

Found that imperfections had a critical impact on the overall AMC performance

1. Alignment errors reduce the bandwidth and increase losses because there is more incoherent scattering

2. Maintaining precision of smoothness/uniformity of all exterior surfaces of slab decreased losses

3. Need enough copper in the reference to achieve a an adequate reference plane

An artificial magnetic conductor has been realized with Capacitively Loaded Loops (CLLs)

Dimensions of each CLL element

W = 160 mils
L = 100 mils
U = 65 mils
S = 49 mils
T = 18 mils

100 mils = 2.54mm < λ_0 / 10

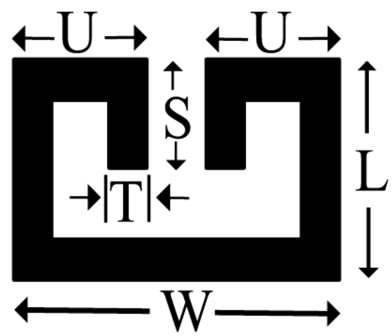

CLL elements have been used successfully in U Arizona DNG metamaterial studies

A. Erentok, P. Luljak, and R. W. Ziolkowski, *IEEE Trans. Antennas and Propagat.*, vol. 53, pp. 160-172, Jan 2005

Metamaterial-based AMC block has been designed, fabricated and measured

No Ground Plane

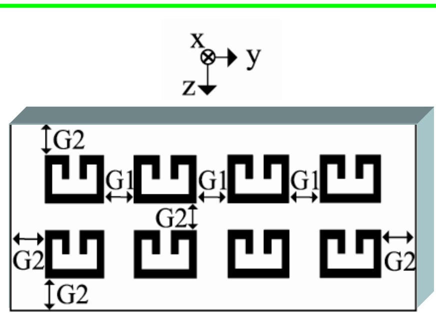

Acts like PMC

CLL-based AMC block

Acts like PEC

Two CLL-deep unit cell geometry

G1= 40 mils = 1.016 mm G2=20 mils =0.508 mm

Unit cell size

31 mils x 800 mils x 260 mils

(0.7874 mm x 20.32 mm x 6.604 mm)

Finite versions of the HFSS designs were simulated, fabricated and measured. The AMC block was formed with a stack of 31 unit cells.

Block diagram

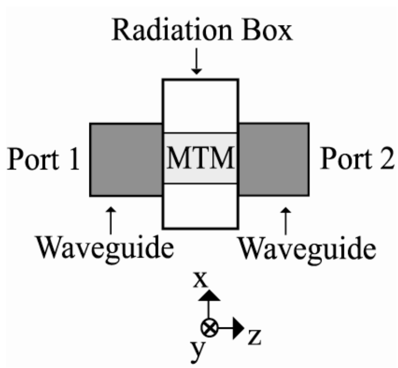

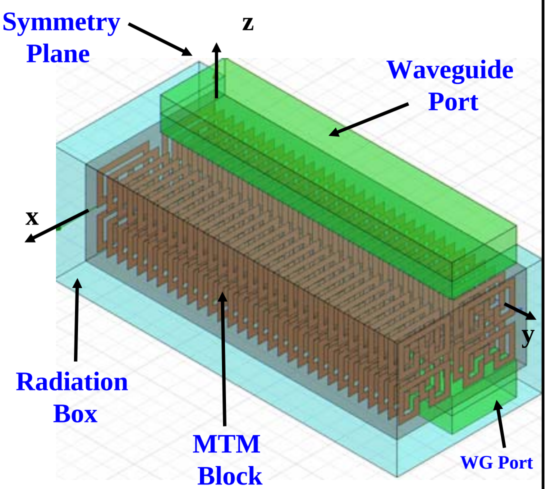

- **The HFSS simulation space closely modeled the experimental setup: the MTM block was sandwiched between two X-band waveguides**

The phase of the AMC block was measured in reference to a PEC plate

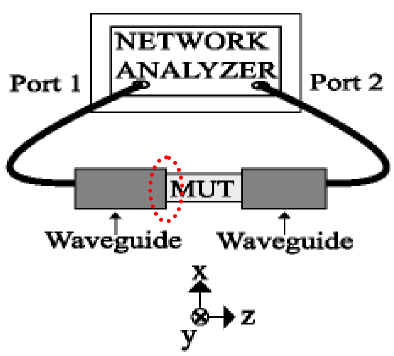

The S-parameters were measured with an HP-8720C network analyzer

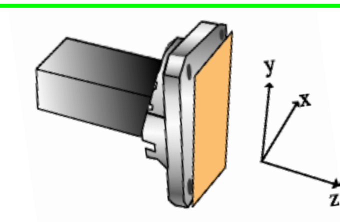

PEC Reference

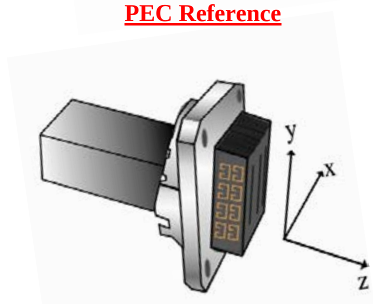

AMC Block

Volumetric AMC block without ground plane designed and tested

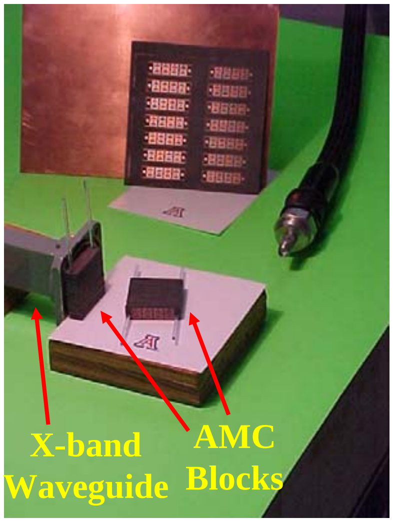

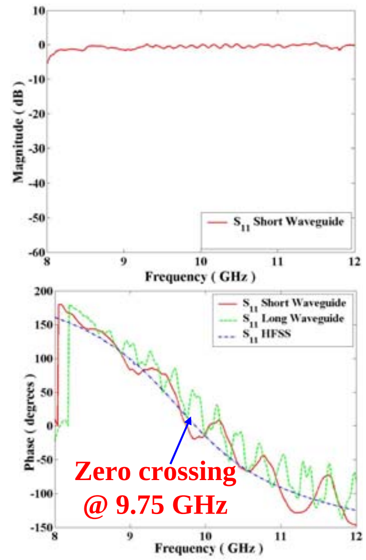

Measured Zero Phase crossing is 1.02% different from the predicted value

Erentok, P. Luljak, and R. W. Ziolkowski, IEEE AP Special Issue on AMCs, *IEEE Trans. Antennas and Propagat.*, vol. 53, pp. 160-172, January 2005.

A 4x4 CLL unit cell was also used in HFSS simulations

Acts like PMC

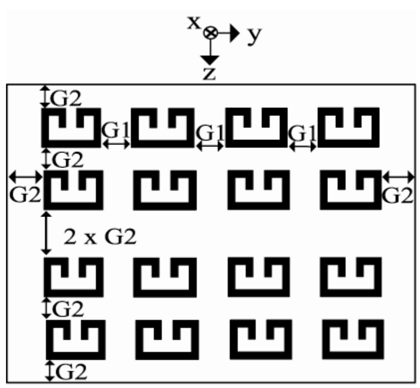

Acts like PEC

Four CLL-deep unit cell geometry

G1= 40 mils G2=20 mils

Unit cell size

31mils x 800mils x 520 mils

Several 4x4 CLL-deep unit cell structures were investigated using HFSS simulations

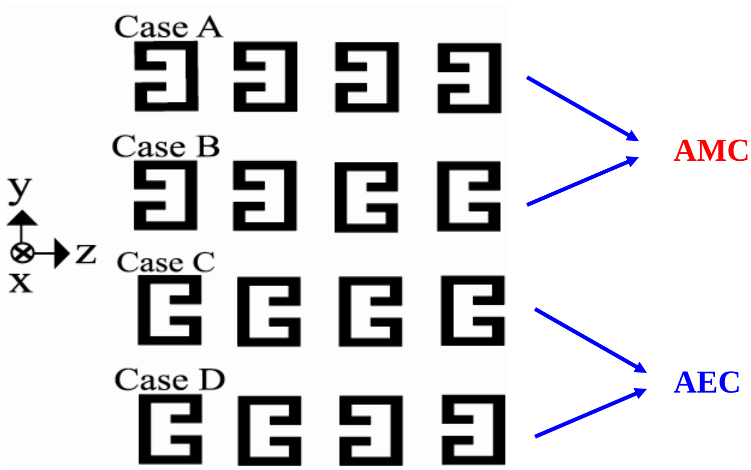

The magnitudes and phases of the HFSS predicted S_{11} values for the four CLL-deep unit cell

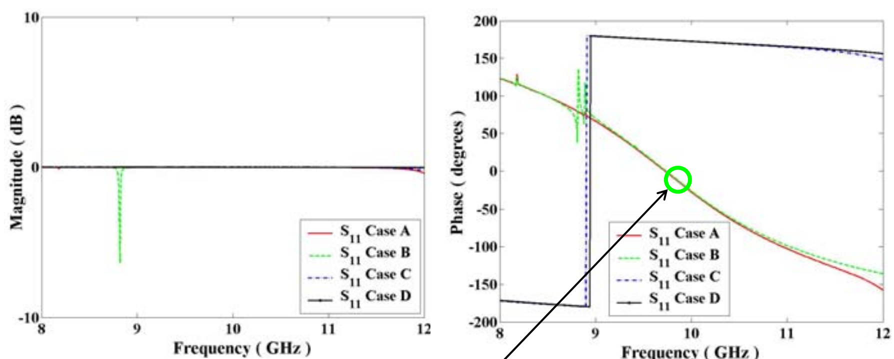

The zero phase crossing of the HFSS predicted S_{11} value for the cases *A* and *B* occurs at 9.73 GHz

The magnitudes and phases of the experimentally measured S_{11} values for the finite four CLL-deep MTM blocks show the predicted high reflectivity over the X-band frequencies

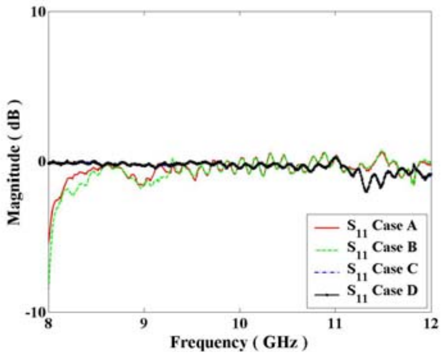

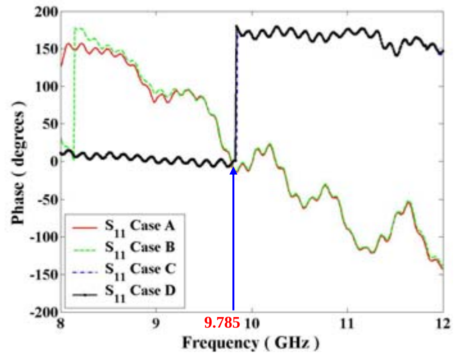

The zero phase crossing of the measured S_{11} values for the cases *A* and *B* occurs at 9.785 GHz, 0.5653% different from the predicted value

Single CLL Unit Cell was simulated with HFSS to extract the permittivity and permeability

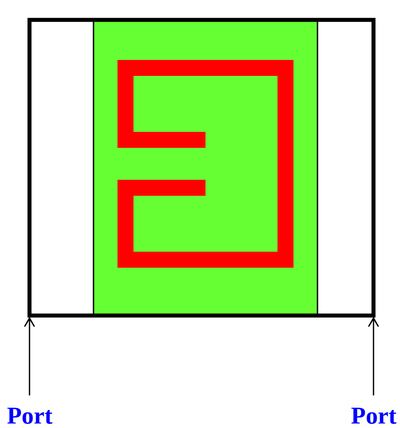

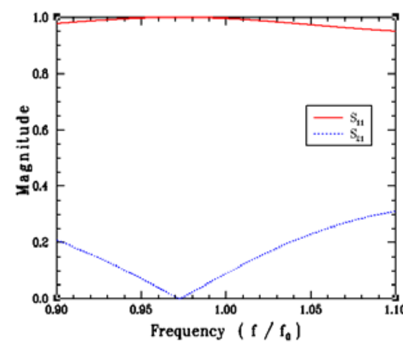

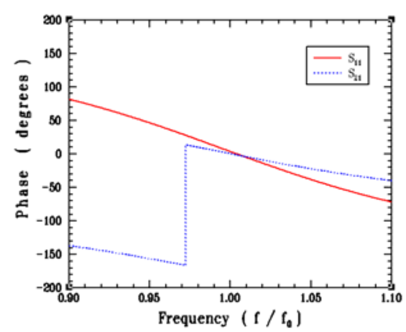

The matching permeability indicates a 2TDLM behavior; the matching permittivity indicates a Drude behavior

Permeability

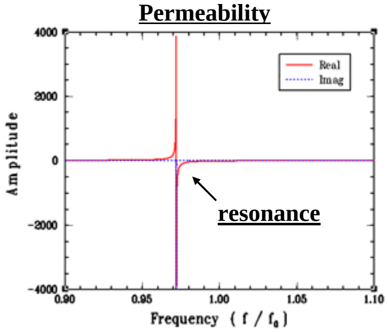

Permittivity

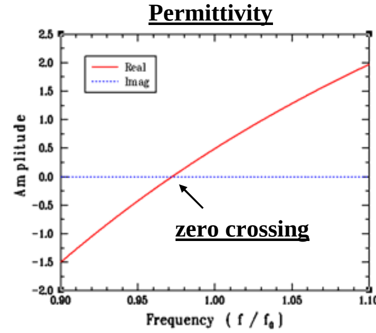

$$\mu(\omega) = \mu_0\left(1 + \frac{\chi_{\alpha m}\omega_{pm}^2 + j\chi_{\beta m}\omega_{pm}\omega - \chi_{\gamma m}\omega^2}{-\omega^2 + j\Gamma_m\,\omega + \omega_{0m}^2}\right)$$

$$f_{0m} = 0.97\,GHz$$

$$\omega_{pm} = \omega_{0m},\ \chi_{\alpha m} = 0.3, \chi_{\beta m} = 10^{-5},$$

$$\chi_{\gamma m} = -0.5, \Gamma_m = 10^{-5}\,\omega_{0m}$$

$$\varepsilon(\omega) = 9\varepsilon_0\left(1 + \frac{\omega_{pe}^2}{-\omega^2 + j\Gamma_e\,\omega}\right)$$

$$f_{0e} = 0.97\,GHz$$

$$\omega_{pe} = \omega_{0e},\quad \Gamma_e = 10^{-5}\,\omega_{pe}$$

Fit by brute force

There is reasonable agreement between the matched models and the corresponding S-parameters

The magnitude is easier to fit than the phase

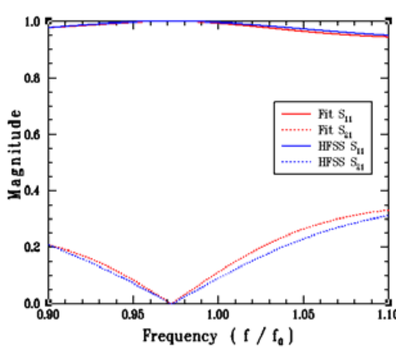

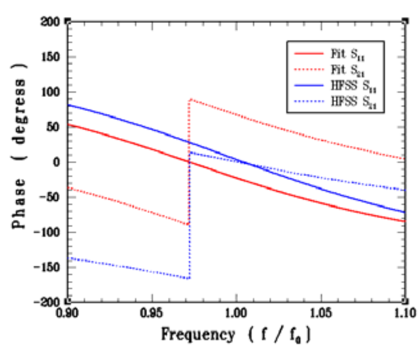

Thus, at the target frequency the AMC block has:

$\mu \to \infty, \varepsilon \to 0$ so that $\eta \to \infty$

2TDLM and Drude models were used is a model-based parameter estimation to match the HFSS-predicted magnitude and phase values of the S_{11} and S_{21} parameters for a unit cell CLL element

2TDLM (Permeability)

$\chi\alpha$	: (variable) [0.1,2]	
$\chi\gamma$	: (variable) (-1,1]	
$\chi\beta$	: (fixed) 1e-4	
Lm	: (variable) [0,10]	Background weighting
Γm	: (fixed) 1e-5 * ωpm	
ωom	: (variable) [9,11] GHz * 2π	
ωpm	: (fixed) 10 * 2π GHz	

Drude Model (Permittivity)

ωpe	: (variable) [9,11] GHz * 2π	
Γe	: (fixed) 1e-5 * ωpe	Background weighting
Le	: (variable) [0,10]	

- ✓ The total number of variables are 6
- ✓ The initial parameter values are randomly selected between [0,1], and these values normalized to the defined boundaries.

The 2TDLM and Drude model parameters were optimized by fitting the S_{11} and S_{21} values to the corresponding HFSS simulation results

- ➢ The optimization results were obtained using 2001 discrete frequency points between 9 and 11 GHz

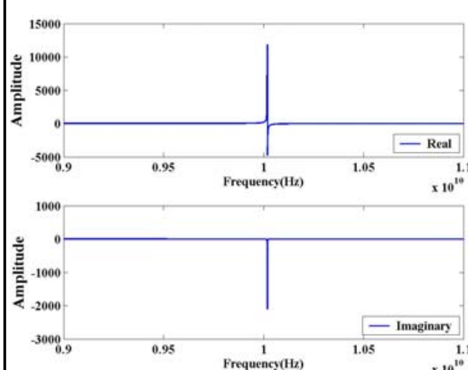

Permeability Values

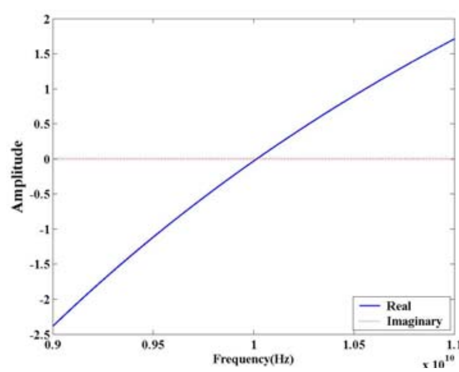

Permittivity Values

MATLAB Optimization Toolbox default values were modified to obtain the most accurate results

- ➢ MATLAB optimization toolbox default settings were modified, e.g., maximum error tolerance = 1e-12, maximum function error tolerance = 1e-12
- ➢ The number of the function iterations is increased from 1e4 to 1.5e6

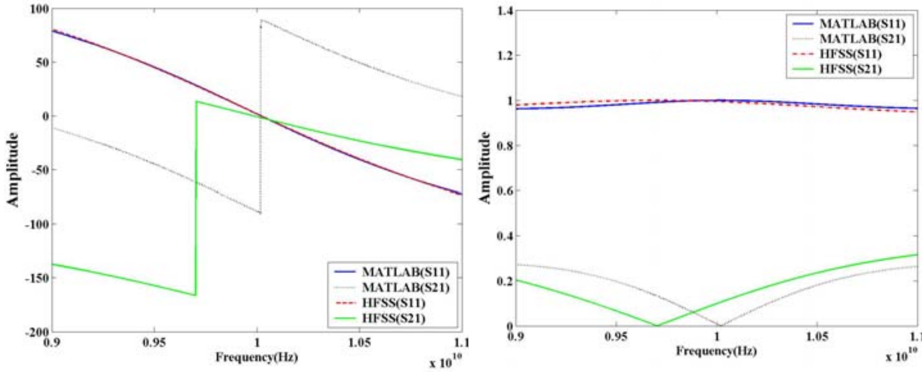

✓ The obtained fitness value is 0.58186 *(Best Result)*

✓ The best fit was obtained using S_{11} values only

Brute Force vs. MATLAB Optimization Toolbox Results shifted to 9.70 GHz resonance and zero crossing

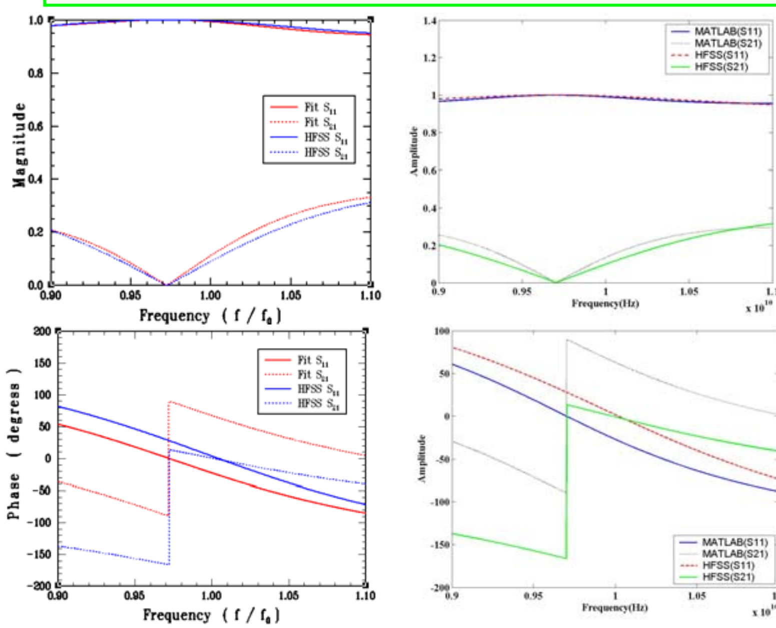

Modeled-based Parameter Estimation CONCLUSIONS

- ✓It is difficult to obtain a perfect match for *both* S_{11} and S_{21}, magnitude and phase values using the 2TDLM and Drude Models. The best convergence value is obtained using only S_{11} values to fit the 2TDLM and Drude models.

The S_{11} phase values required f_{pm} and f_{om} frequencies to be 10 GHz for best match.
The S_{21} magnitude & phase values required f_{pm} and f_{om} to be 9.702 GHz for best match.

- ✓ The optimization scenarios using 2TDLM model for both permittivity and permeability values did not converge (to the correct values)
- ✓ The S_{11} phase values strictly depend on Γ_β. The optimization results suggest that the upper value of the Γ_β should be restricted to 0.0001.
- ✓ The proportionality constant of the Drude model also had a big impact on the matched S_{11} phase and magnitude values. The optimization results showed that the proportional constant should be restricted to the small numbers, e.g., [0,15] to prevent $|S_{11}|$ values from becoming flat and equal to 1.

Artificial Magnetic Conductors (AMCs) provide important advantages for antenna applications

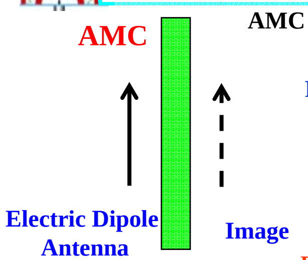

AMC doubles a nearby electric dipole rather than shorting it out

Potential antenna applications include
- Low-profile antenna design
- Improved radiation pattern (both in near- and far-field)
- Reduced mutual coupling in multiple antenna systems

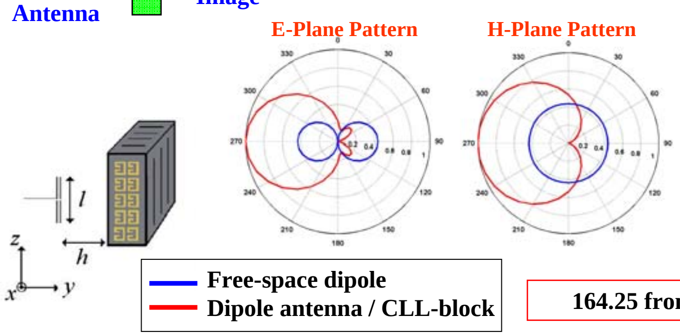

- $h = \lambda_0 / 25$
- $f = 9.987$ GHz

164.25 front-to-back ratio !

A. Erentok, P. Luljak, and R. W. Ziolkowski, *IEEE Trans. Antennas and Propagat.*, vol. 53, pp. 160-172, Jan 2005

The resonance between the dipole and the AMC block also produces enhanced near field performance

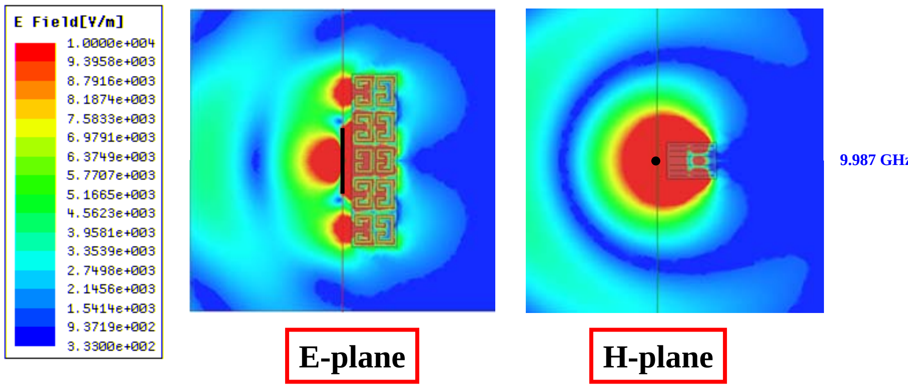

Erentok, P. Luljak, and R. W. Ziolkowski, IEEE AP Special Issue on AMCs, *IEEE Trans. Antennas and Propagat.*, vol. 53, pp. 160-172, January 2005.

Metamaterials (MTMs) have exotic properties that may have a high impact on a wide variety of practical applications

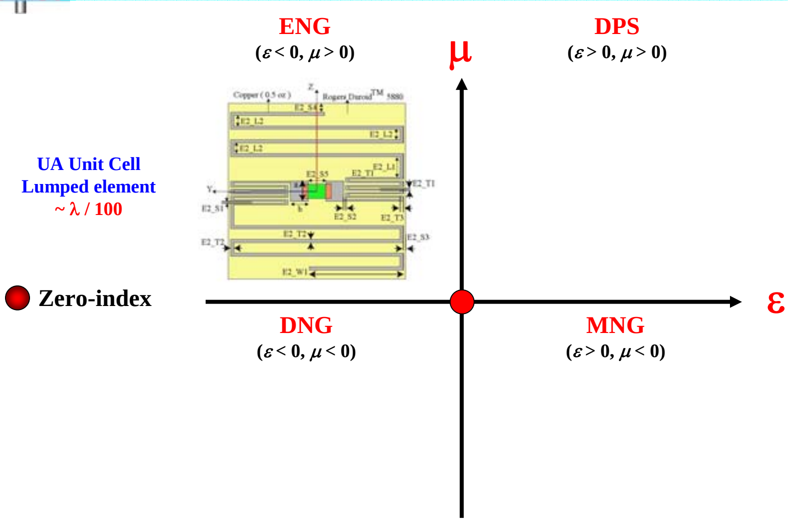

“Re-discovery of bed-of-nails medium for ENG effects

Walter Rotman, 1961; Pendry et al 1996

Two-dimensional anisotropic lattice

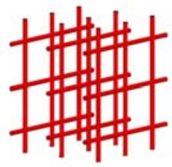

Three-dimensional anisotropic lattice

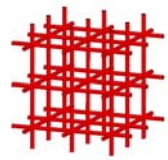

Three-dimensional isotropic lattice

$$\varepsilon_p = \varepsilon_0 \left(1 - \frac{\omega_p^{\ 2}}{\Gamma^2 + \omega^2} + j\,\frac{\omega_p^{\ 2}\,\Gamma/\omega}{\Gamma^2 + \omega^2} \right)$$

ω_p	is the plasma frequency
Γ	is the collision frequency
ε_0	permittivity of free space

NOTE: “infinite” wires required

Finite Element Simulator

HFSS simulations

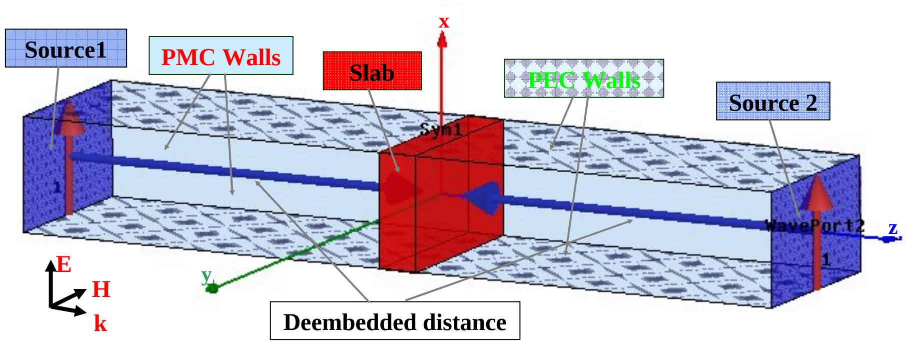

Extract material parameters from reflection and transmission results

Pascal Imhof, MS Thesis, 2006, EPFL, LEMA

Cylindrical and rectangular PEC wire medium models that exhibit the desired effective medium properties

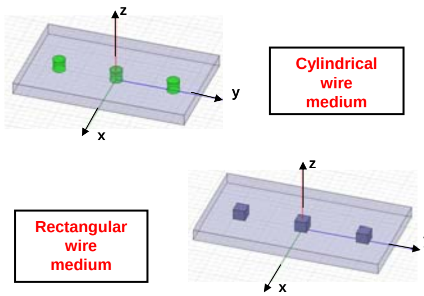

Drude behavior

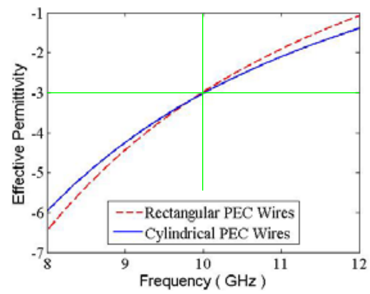

Wire structures

Extracted permittivities

Surface area of the inclusions and the spacing between them govern the plasma frequency

Cut wires

do not produce ENG properties at low frequencies

ENG MTM TESTING

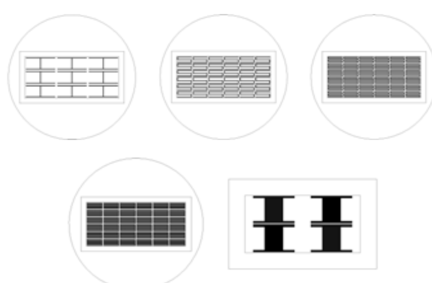

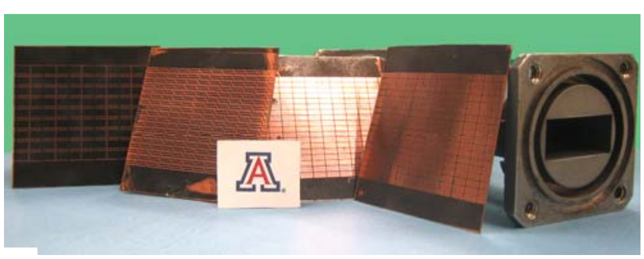

Pascal Imhof, MS Thesis, 2006, EPFL, LEMA

Measurements (1)

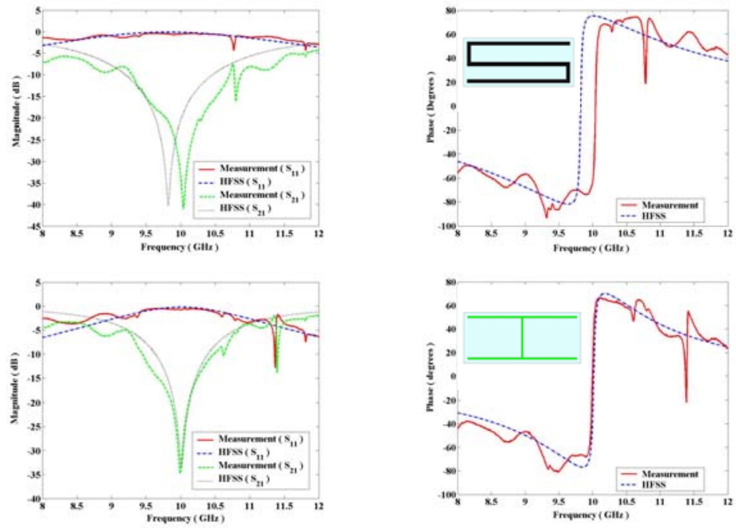

Pascal Imhof, MS Thesis, 2006, EPFL, LEMA

Measurements (2)

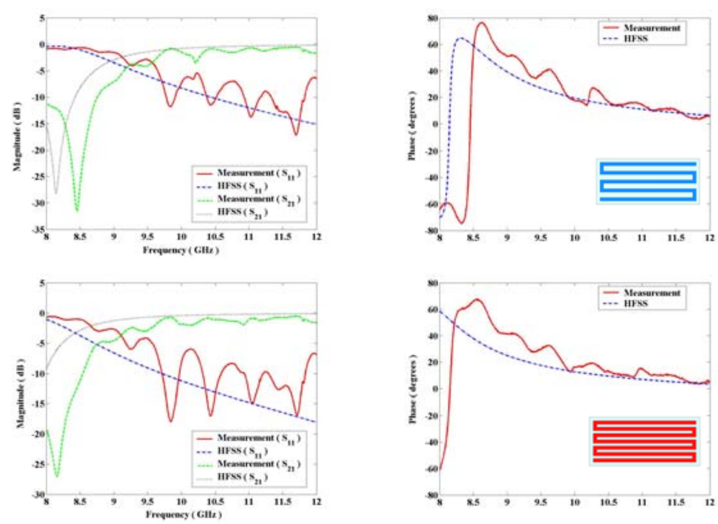

Pascal Imhof, MS Thesis, 2006, EPFL, LEMA

Design of highly subwavelength ENG unit cells

Pascal Imhof, MS Thesis, 2006, EPFL, Supervisors Profs. J. Mosig and R. W. Ziolkowski

Meander line
ε_r=-3 @ 2.554 GHz
$\lambda_0/100 \times \lambda_0/100$

Lumped element - S line
ε_r= -2.96 –j 0.093 @ 430 MHz
$\lambda_0/331 \times \lambda_0/681$

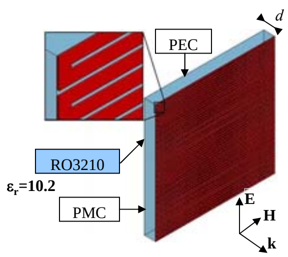

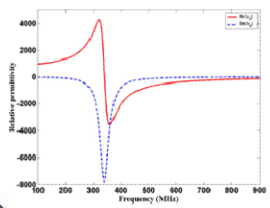

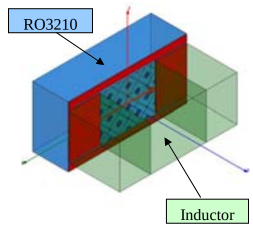

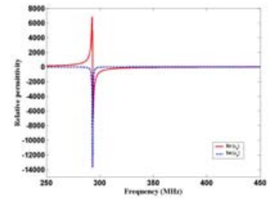

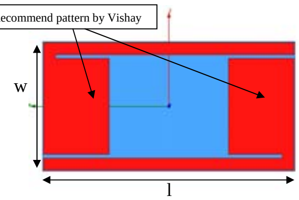

w=1.0246mm
l=2.1082mm

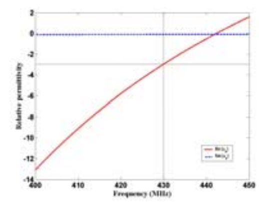

Highly isotropic structures

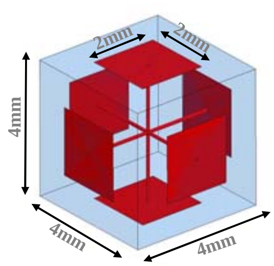

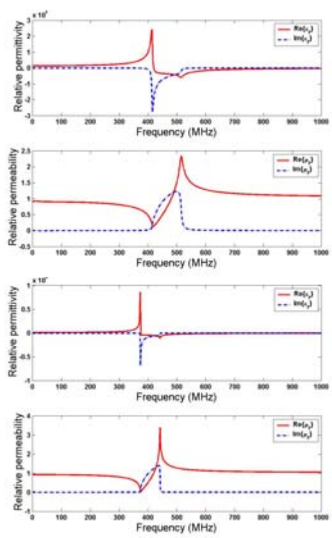

Pascal Imhof, MS Thesis, 2006, EPFL, LEMA

Metamaterials (MTMs) have exotic properties that may have a high impact on a wide variety of practical applications

ENG ($\varepsilon < 0$, $\mu > 0$)

DPS ($\varepsilon > 0$, $\mu > 0$)

μ

● Zero-index

ε

DNG ($\varepsilon < 0$, $\mu < 0$)

MNG ($\varepsilon > 0$, $\mu < 0$)

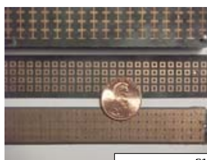

UA Low Loss DNG and SNG X-band elements

~ -0.3dB/cm

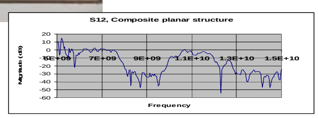

DNG MTMs are achieved by combining MTMs with ENG and MNG effects in the same frequency regime

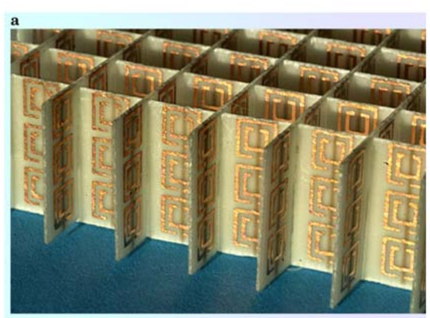

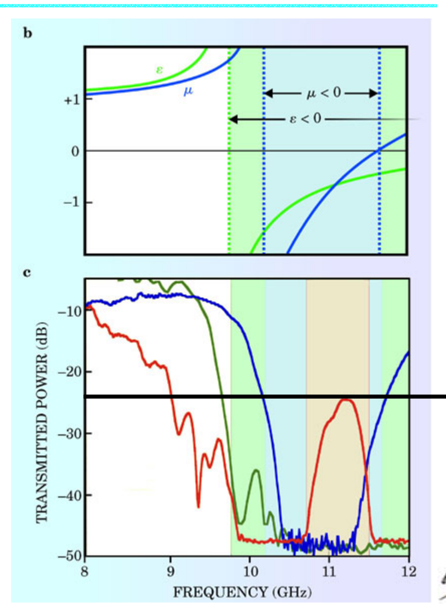

UCSD Experiments
David Smith, Shelly Schultz, et al.

UA DNG MTM was designed to achieve a matched medium at 10 GHz

Electric dipole metamaterial

ENG

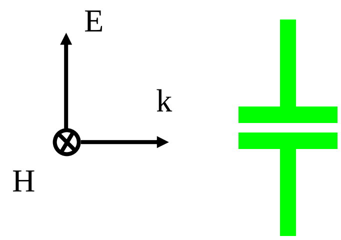

Capacitively Loaded Strip (CLS) Unit element

Magnetic dipole metamaterial

MNG

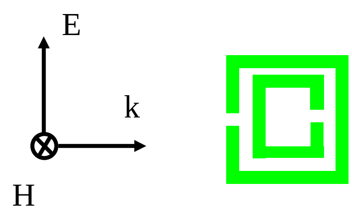

Split Ring Resonator (SRR) Unit element

R. W. Ziolkowski, IEEE Trans. AP, vol. 51, pp. 1516-1529, July 2003

Compact metamaterials having negative index of refraction have been designed, fabricated and tested experimentally

- All structures constructed with Rogers Corporation
  5880 Duroid (ε_r = 2.2, μ_r = 1.0, tan d = 0.0009)
  31 mil (100 mil = 2.54 mm) thick,
  125 mil polyethylene spacers
- S-parameters measured with a free space measurement system at X-band frequencies
- Experimental results confirm the realization of DNG MTMs that are matched to free space
- Very good agreement between numerical and experimental results

The CLS- and SRR-based MTMs were measured separately

Dipoles Only

Split rings only

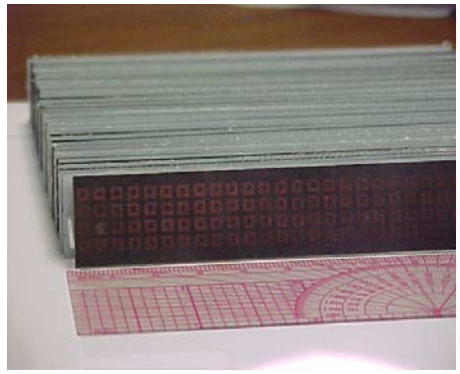

MTM block covers the aperture of an X-band rectangular horn

HFSS was used to design each MTM structure

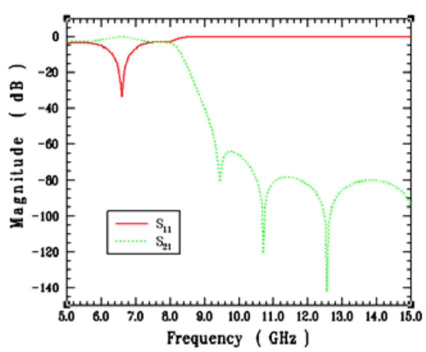

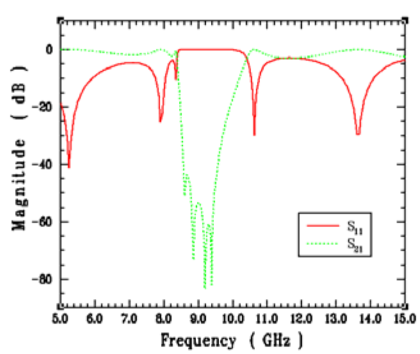

CLS-only MTM

SRR-only MTM

Measurements confirmed the HFSS simulation results showing the DNG medium effects for the planar structure

Dipoles, split rings, & composite planar structure

Free space measurement system

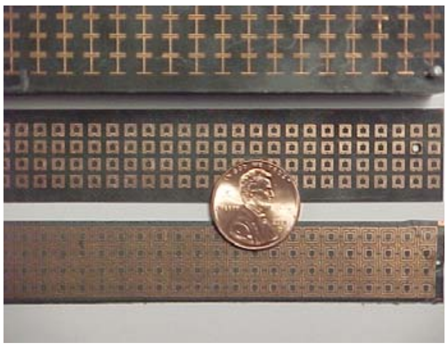

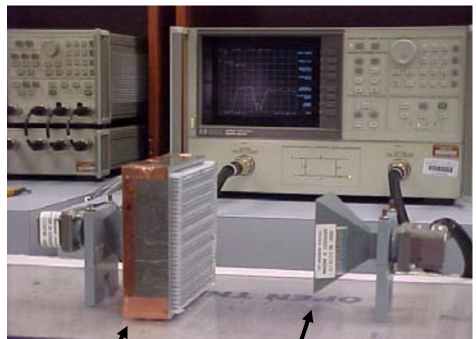

MTM block **X-band horn**

The S_{21} experimental data shows the predicted reflection bands for the electric and magnetic dipole metamaterials

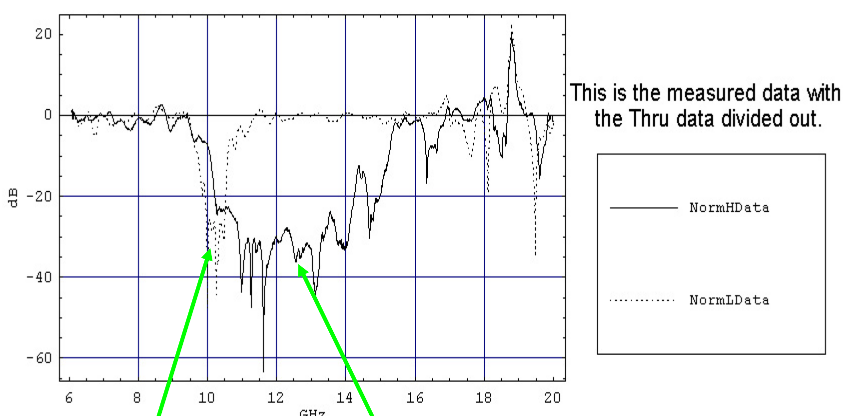

MNG band

ENG band

UA DNG MTM was designed to achieve at 10 GHz a matched-to-free-space medium

Electric dipole metamaterial

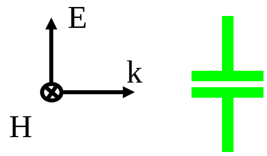

Capacitively Loaded Strip (CLS) Unit element

Finite everything
d ~ λ/10

Magnetic dipole metamaterial

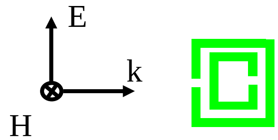

Split Ring Resonator (SRR) Unit element

DNG
Unit Cell Set
Integrated
Planar

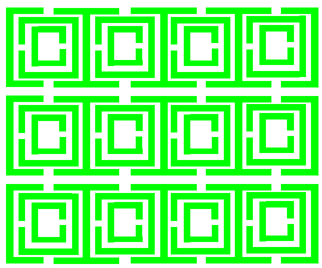

R. W. Ziolkowski, IEEE Trans. AP, vol. 51, pp. 1516-1529, July 2003

HFSS / FDTD Simulation Region

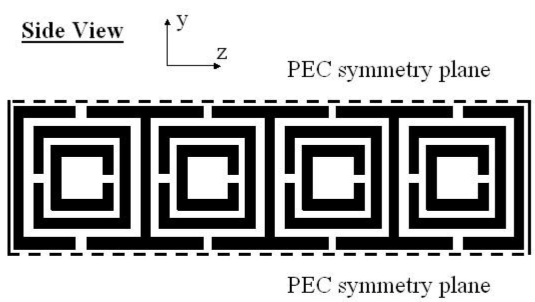

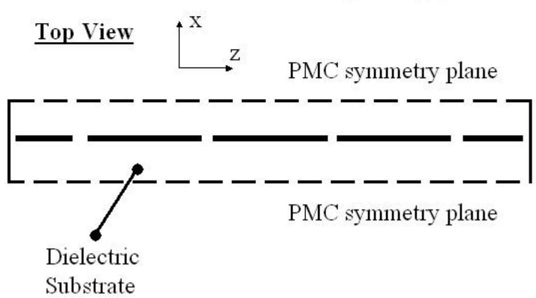

The composite planar MTM S-parameters were calculated with Ansoft's HFSS

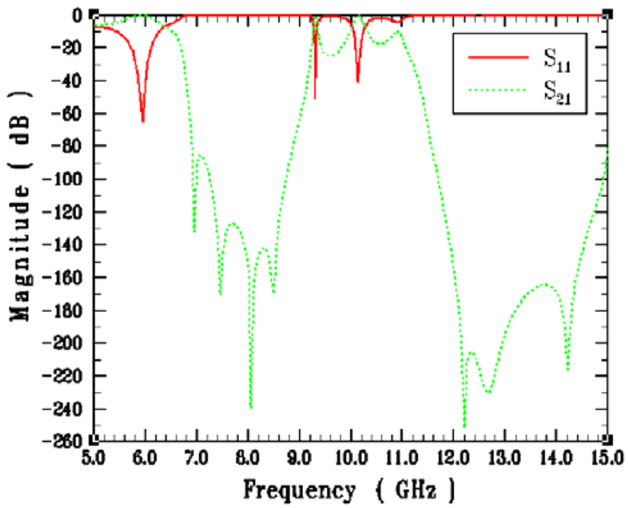

The composite planar MTM S-parameters were calculated with Ansoft's HFSS

Matched frequencies

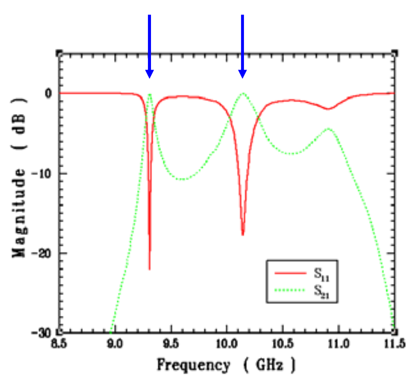

Matched frequencies

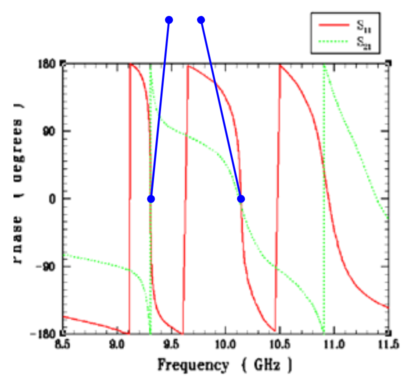

The composite planar MTM exhibits matching to free space in two frequency regions (and nearly three)

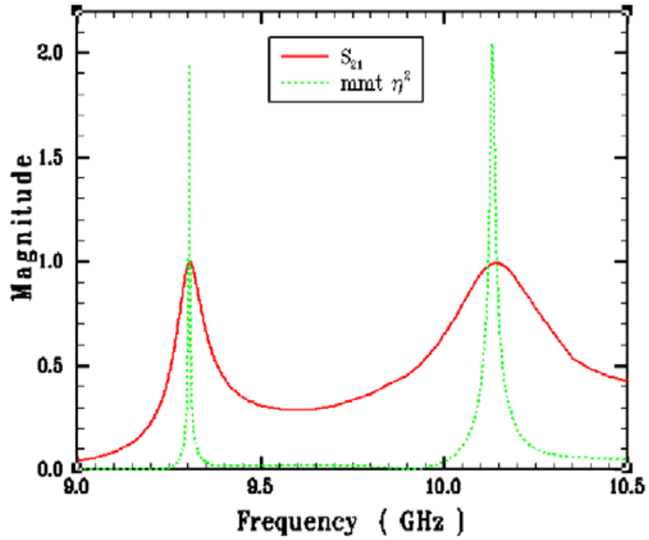

The S_{21} experimental data shows the predicted transmission bands for the matched DNG medium

Loss < 0.3dB/cm

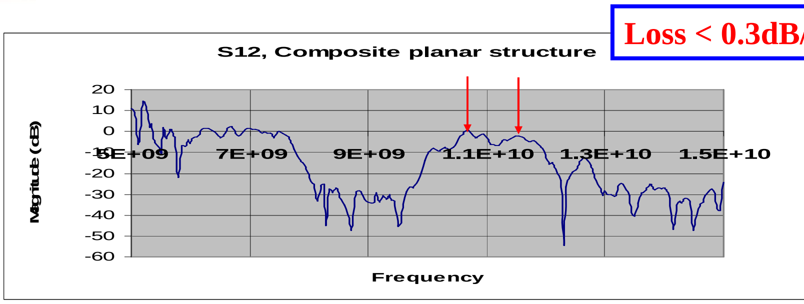

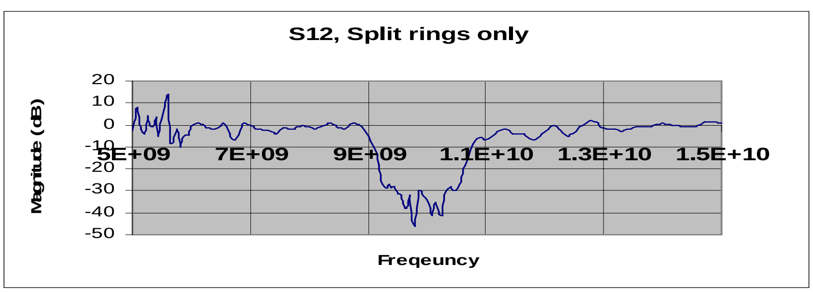

What is more fundamental: ε, μ or n, η ????

$$k = \omega\sqrt{\varepsilon}\sqrt{\mu} = \frac{\omega}{c}n$$

$$n = \sqrt{\frac{\varepsilon}{\varepsilon_0}}\sqrt{\frac{\mu}{\mu_0}}$$

$$\eta = \frac{\sqrt{\mu}}{\sqrt{\varepsilon}}$$

$$\boxed{\begin{aligned} n_{DNG} &= \sqrt{\varepsilon_r}\sqrt{\mu_r} = \sqrt{-|\varepsilon_r|}\sqrt{-|\mu_r|} = \left(-j\sqrt{|\varepsilon_r|}\right)\left(-j\sqrt{|\mu_r|}\right) \\ &= -\sqrt{|\varepsilon_r|}\sqrt{|\mu_r|} \end{aligned}}$$

Index, wave impedance are derived quantities

Can you get negative refraction without DNG media?
Yes – with EBG/PBG media

Effective permittivity and permeability parameters are commonly extracted from S-parameter (calculated/measured) values using the Nicolson, Ross, and Weir approach

$$V_1 = S_{21} + S_{11}$$
$$V_2 = S_{21} - S_{11}$$

$$X = \frac{1 + V_1 V_2}{V_1 + V_2}$$
$$Y = \frac{1 - V_1 V_2}{V_1 - V_2}$$

$$Z = \exp(ikd) = X \pm \sqrt{X^2 - 1}$$
$$\Gamma = Y \pm \sqrt{Y^2 - 1}$$

$$k_0 = \frac{\omega}{c}$$

$$\sqrt{\varepsilon_r \mu_r} = \frac{\ln(Z)}{jk_0 d}$$

$$\sqrt{\frac{\mu_r}{\varepsilon_r}} = \frac{1+\Gamma}{1-\Gamma}$$

$$\mu_r = \frac{1+\Gamma}{1-\Gamma}\frac{\ln(Z)}{jk_0 d}$$

$$\varepsilon_r = \frac{1-\Gamma}{1+\Gamma}\frac{\ln(Z)}{jk_0 d}$$

The effective permittivity and permeability parameters were extracted from the S-parameter values using a modified version of the Nicolson, Ross, and Weir approach

$$\exp(ikd) = \frac{V_1 - \Gamma}{1 - \Gamma V_1}$$

$$\Gamma = \frac{\exp(ikd) - V_2}{1 - V_2 \exp(ikd)}$$

$$1 - \exp(ikd) = \frac{(1 - V_1)(1 + \Gamma)}{1 - \Gamma V_1}$$

$$\sqrt{\frac{\mu_r}{\varepsilon_r}} = \frac{1 - \exp(ikd)}{1 + \exp(ikd)} \frac{1 - V_2}{1 + V_2}$$

$$\sqrt{\varepsilon_r \mu_r} \approx \frac{1}{jk_0 d} \frac{(1 - V_1)(1 + \Gamma)}{1 - \Gamma V_1}$$

$$\mu_r \approx \frac{2}{jk_0 d} \frac{1 - V_2}{1 + V_2}$$

$$\varepsilon_r \approx \left(\frac{k}{k_0}\right)^2 \frac{1}{\mu_r}$$

$$n = \sqrt{\varepsilon_r}\sqrt{\mu_r}$$

$$\varepsilon_r \approx \mu_r - \frac{2}{jk_0 d} S_{11}$$

"Enhanced Result" when $S_{11} \sim 0$

A simplified MTM was designed to isolate the electric and magnetic elements and the corresponding effects

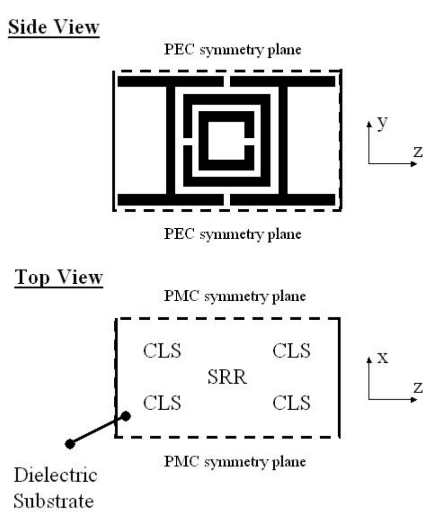

CLS-only MTM

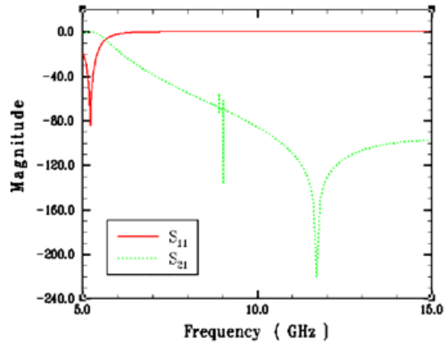

S-parameters, Ansoft's HFSS

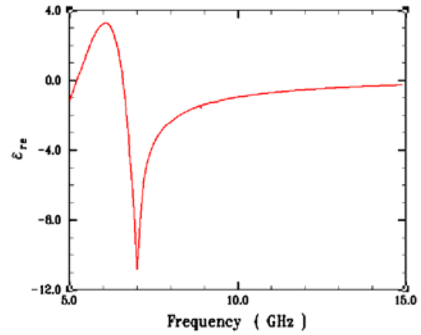

Extracted effective permittivity

SRR-only MTM

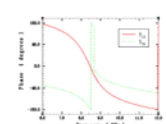

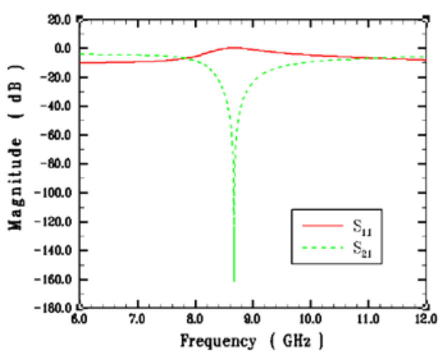

S-parameters, Ansoft's HFSS

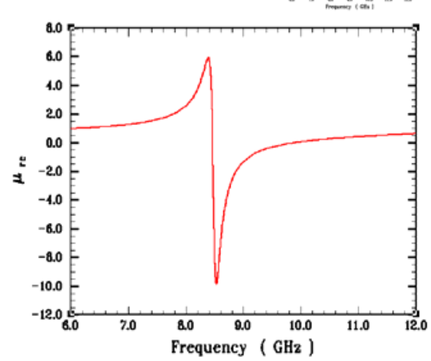

Extracted effective permeability

Composite MTM structure

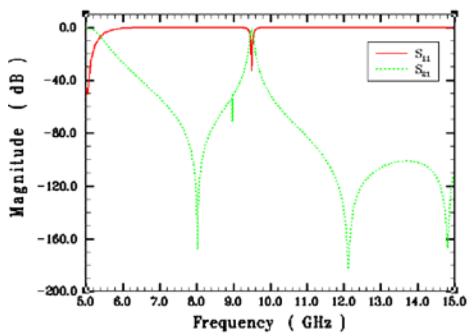

S-parameters, Ansoft's HFSS

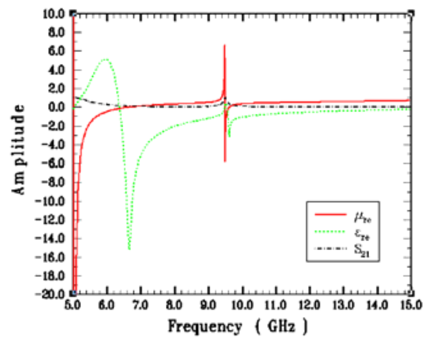

Extracted effective permittivity and permeability

The effective permittivity extraction can be improved near the frequency points matched to free space

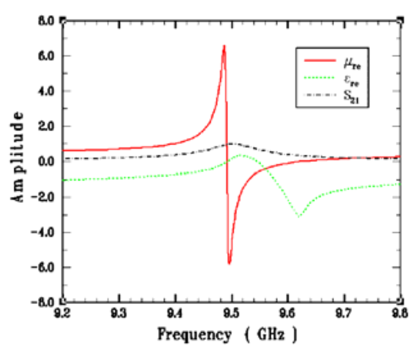

Without enhancements

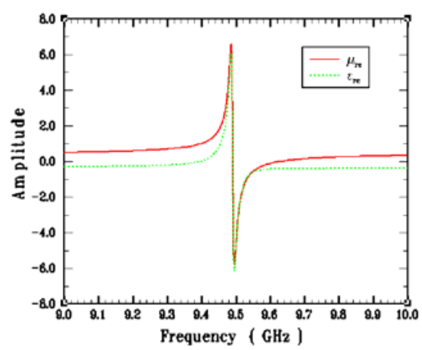

With enhancements

The effective index of refraction of the simplified MTM is negative in the frequency region were matching occurs

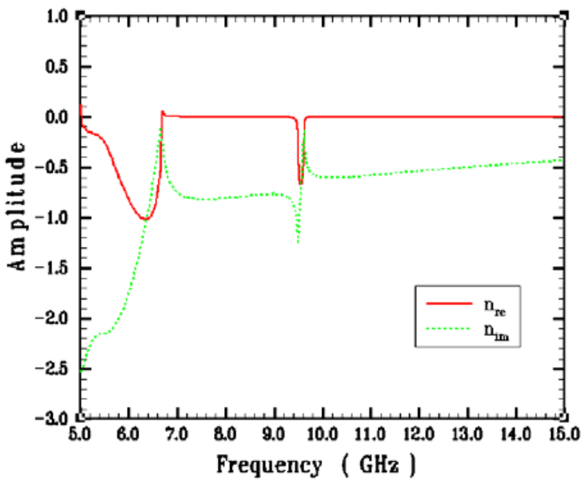

The effective permittivity and permeability of the composite planar MTM were extracted from the HFSS S-parameter calculations

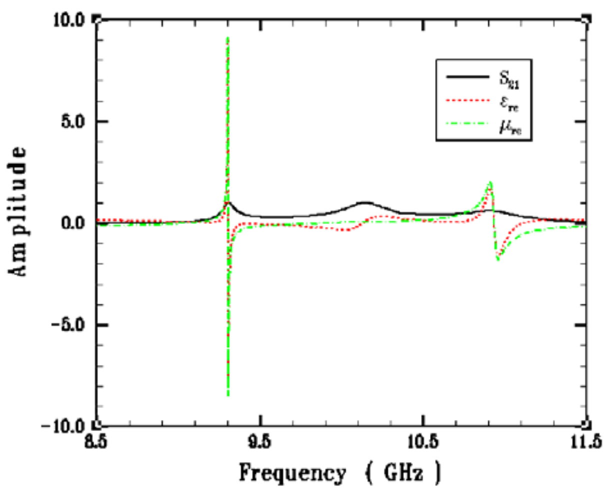

A negative effective index of refraction was extracted from the HFSS S-parameter calculations and from the FDTD calculations

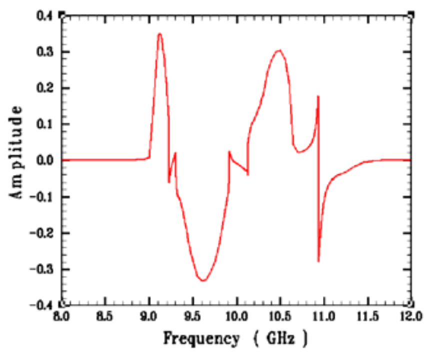

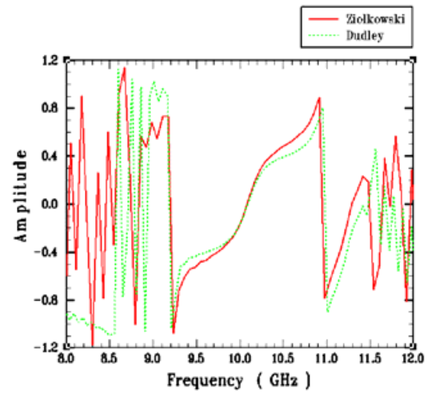

HFSS results

FDTD results

Confirmation that negative index of refraction MTMs was realized

Enhancement of the power radiated by a dipole antenna at boresight by means of a left handed superstrate, E. Sáenz, I. Ederra, R. Gonzalo, P. de Maagt

IWAT 2006

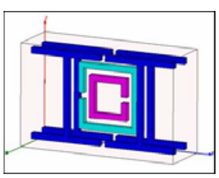

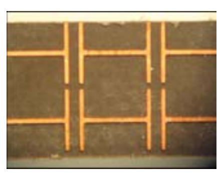

Aperture efficiency with and without superstrate

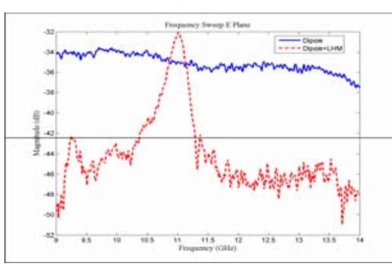

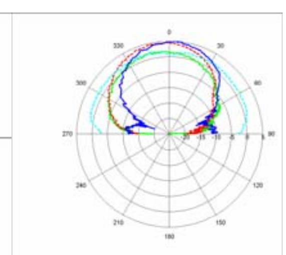

Radiation patterns

Aperture efficiency is larger than one – field at edges of the superstrate make the effective aperture area larger than the physical area

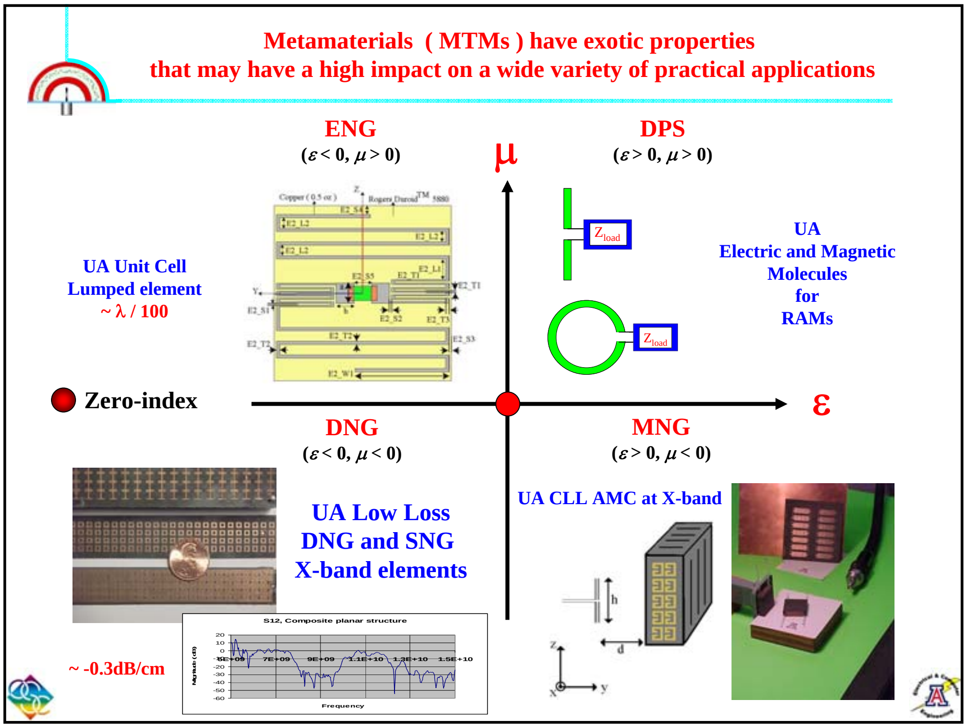
Metamaterials (MTMs) have exotic properties
that may have a high impact on a wide variety of practical applications
ENG
(ε < 0, μ > 0)
μ
DPS
(ε > 0, μ > 0)
UA Unit Cell
Lumped element
~ λ / 100
UA
Electric and Magnetic
Molecules
for
RAMs
Zero-index
ε
DNG
(ε < 0, μ < 0)
MNG
(ε > 0, μ < 0)
UA Low Loss
DNG and SNG
X-band elements
UA CLL AMC at X-band
~ -0.3dB/cm
S12, Composite planar structure
Frequency

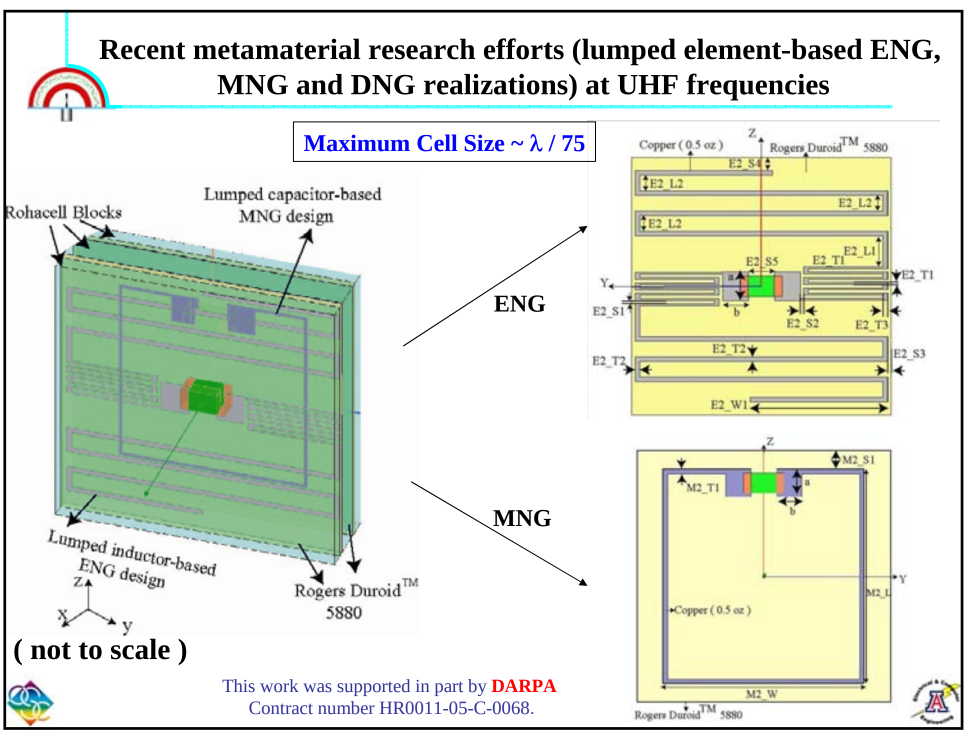
Recent metamaterial research efforts (lumped element-based ENG, MNG and DNG realizations) at UHF frequencies
Maximum Cell Size ~ λ / 75
Rohacell Blocks
Lumped capacitor-based
MNG design
Lumped inductor-based
ENG design
Rogers Duroid™
5880
ENG
MNG
Copper (0.5 oz)
Rogers Duroid™ 5880
(not to scale)
This work was supported in part by DARPA
Contract number HR0011-05-C-0068.

Lumped-element based unit cells have achieved the smallest, lowest frequency ENG, MNG, DNG (NIM) materials to date

$n_{real} = -3.11$ with a loss of 0.91 dB/*cm* at 400 MHz for 10mm, λ /75 unit cell

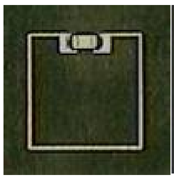

MNG portion

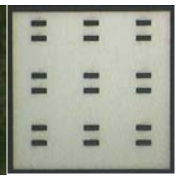

Rohacell^{TM} spacer

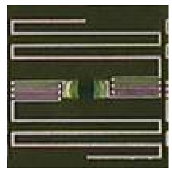

ENG portion

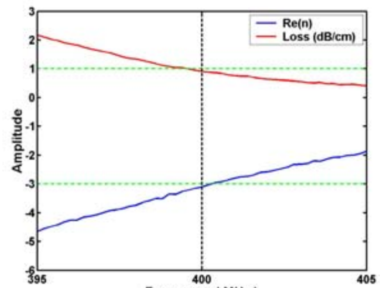

Frequency (MHz)

Complete NIM slab (~ 900 Unit Cells)

(not to scale)

This work was supported in part by **DARPA**
Contract number HR0011-05-C-0068.

Metamaterials (MTMs) have exotic properties that may have a high impact on a wide variety of practical applications

ENG
($\varepsilon < 0, \mu > 0$)

μ

DPS
($\varepsilon > 0, \mu > 0$)

UA Unit Cell
Lumped element
~ λ / 100

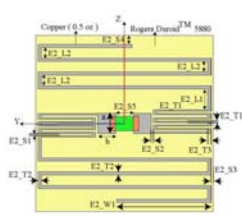

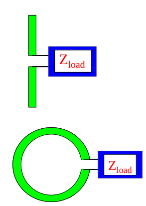

UA
Electric and Magnetic
Molecules
for
RAMs

Zero-index

ε

DNG
($\varepsilon < 0, \mu < 0$)

MNG
($\varepsilon > 0, \mu < 0$)

$n_{real} = -3.11$

loss = 0.91 dB/*cm*
at 400 MHz
for 10mm,
λ /75 unit cell

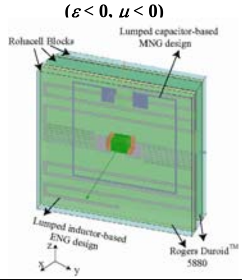

UA CLL AMC at X-band

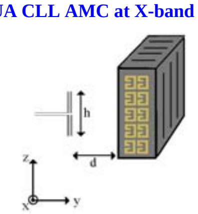

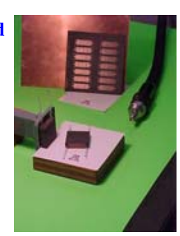

Metamaterials (MTMs) have exotic properties that may have a high impact on a wide variety of practical applications

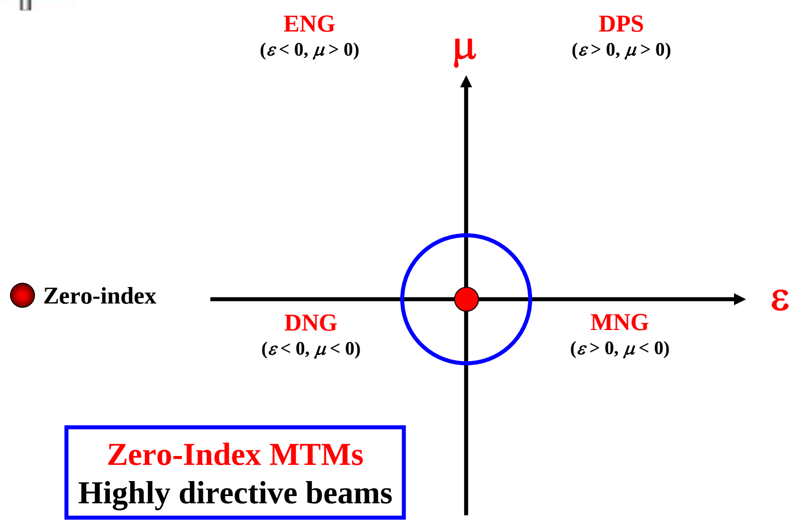

Zero-Index MTMs
Highly directive beams

FDTD-predicted electric field distributions show that a line source in a zero-index slab creates a uniform aperture field leading to a narrow beam profile

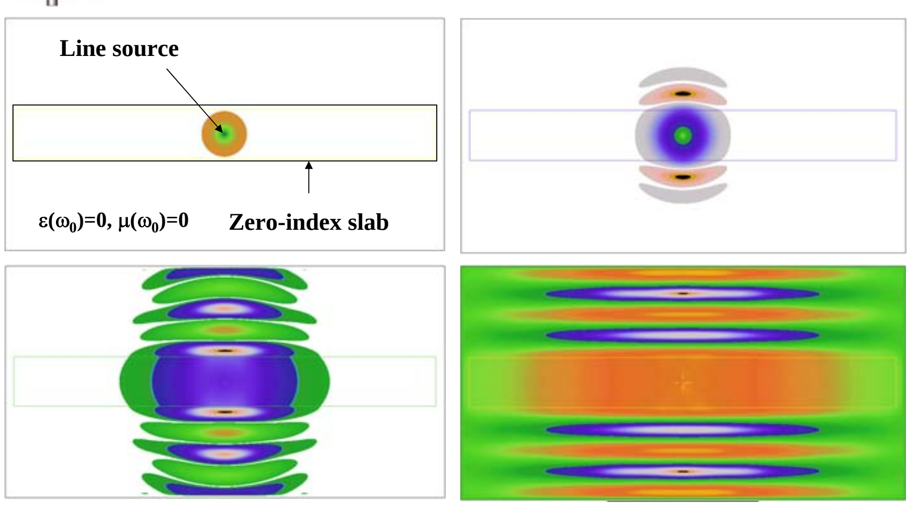

Aperture loaded with field having constant, uniform phase leads to most directive output beam

Ziolkowski, Phys. Rev. E, vol. 70, 046608, October, 2004

Dr. Steve Franson
PhD Dissertation, November 2007
Motorola MMW Divsion

Manuscripts in review

Highly directive antennas
desired for
1km WLAN systems at 60GHz

Zero-n superstrate leads to enhanced antenna gain

Patch antenna driven
3 layer
grid superstrate
structure

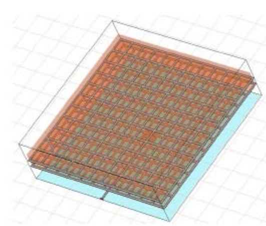

(a) Structure

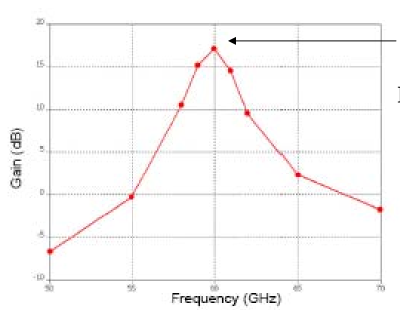

17.2dB

Bare Patch ~ 3.2dB

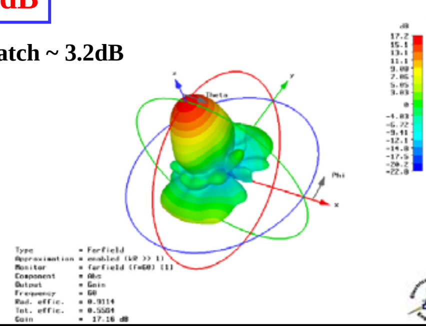

Fabricated 60 mil Period Dipole

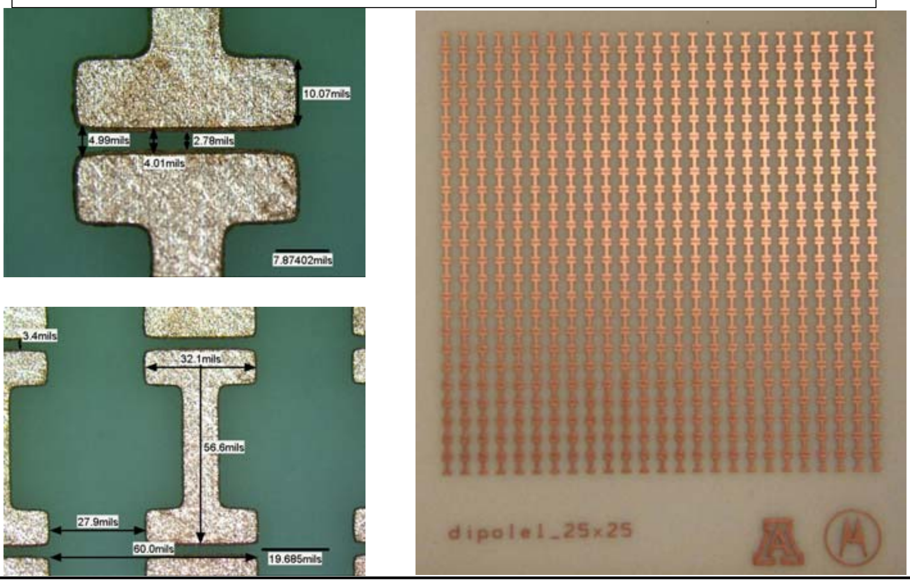

Fabricated 40 mil Period Dipole

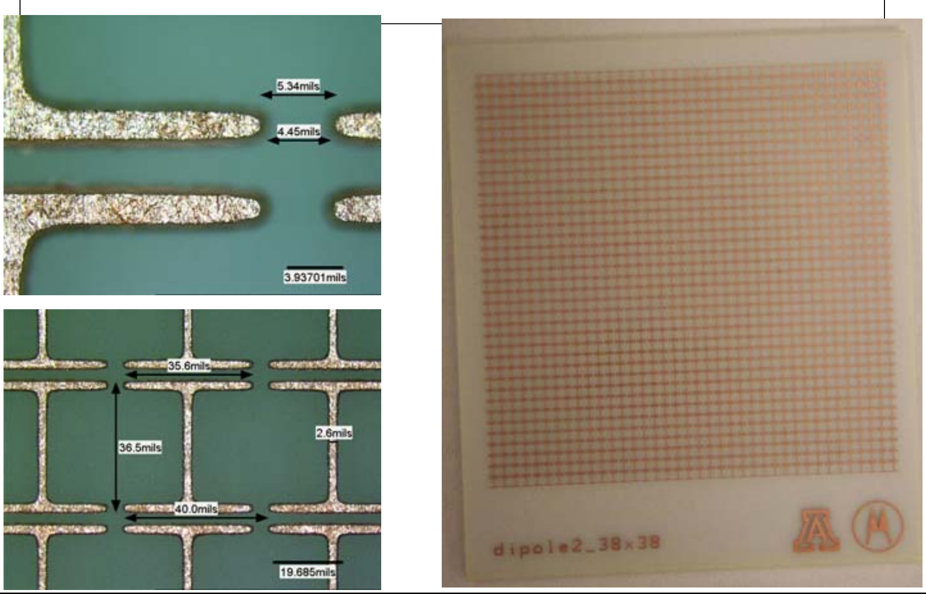

Fabricated 30 mil Period Ring

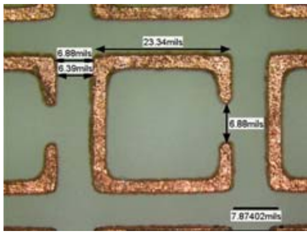

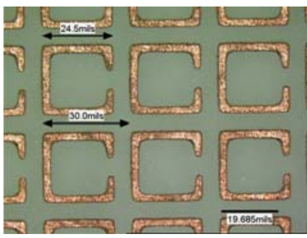

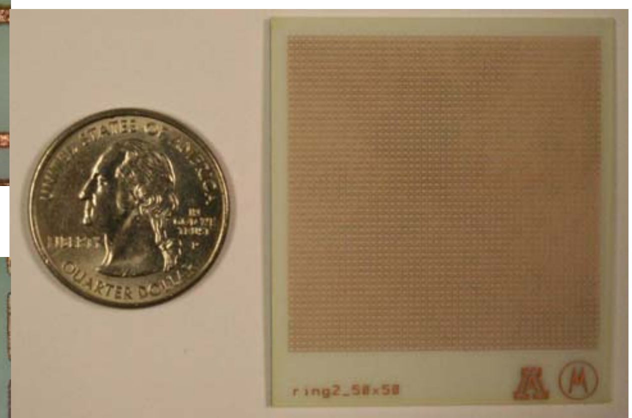

Does the grid have Zero N?

- Matlab code verified a zero index of refraction for a 2 layer infinite grid

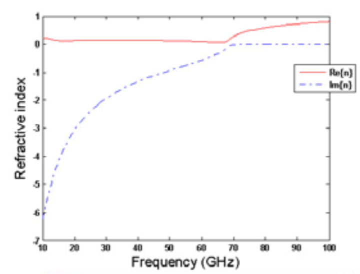

- The simulated phase of the transmitted wave was consistent with Zero N

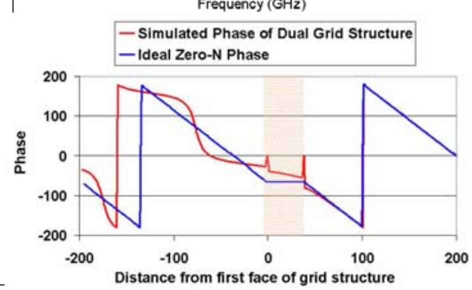

Dipole Superstrate

- Gain = 13.7dBi
- Operating well below resonance
- Acting similar to high dielectric

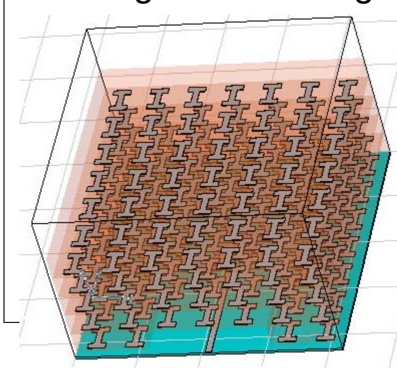

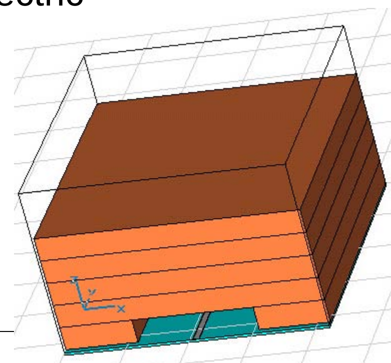

Grid Superstrate

- Nearly 19dBi of simulated Gain
- First Simulated in CST to find best configuration
- Simulated and tuned in XFDTD for high accuracy

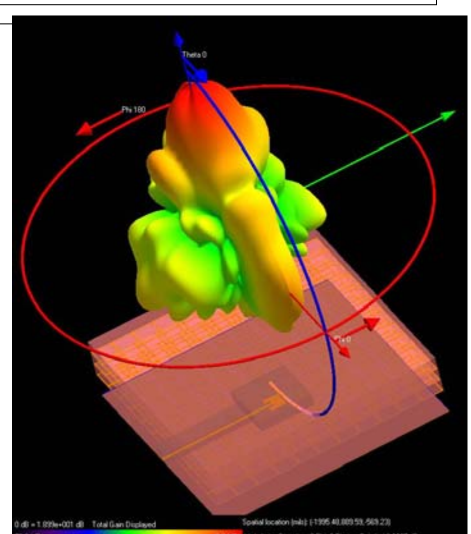

Fabricated Grid

- Dimensions match well with designs

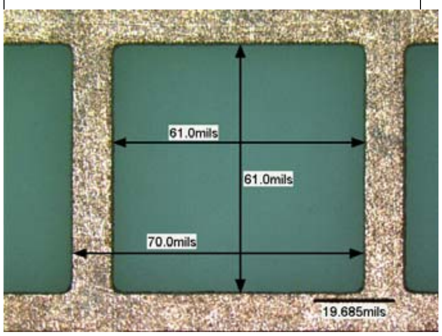

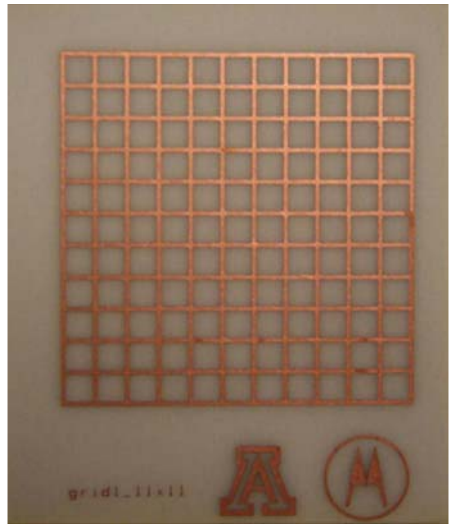

Curvature

- The material is very flexible
- When adhesive backing is removed, significant curvature occurs
- Tape is used to “tune” spacing and curvature

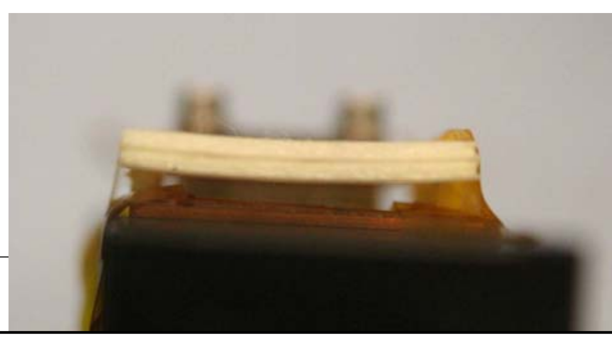

Antenna Construction

- 68 mil period design used a 70 mil thick rigid foam spacer (shown)

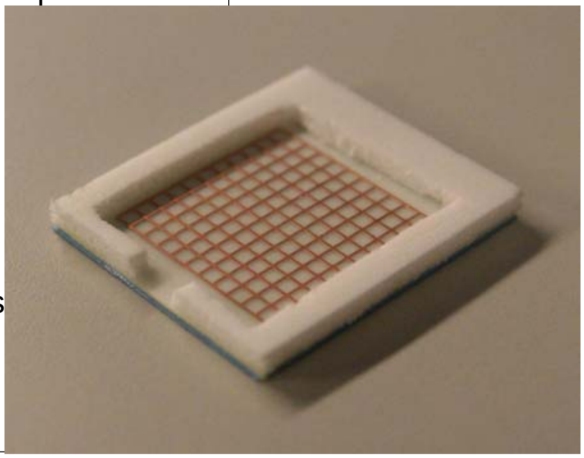

- 70 mil period design used 2 layers of flexible foam (not shown)

Measured Results Information

- All measured results are the system gain of the entire antenna structure, including the feed transmission line
- Tuning was only possible for system gain
- Unlike other antennas, the best system gain frequency was not typically the same as the best gain frequency
- All results are “tuned” for best performance. Tape affects spacing, thickness, and curvature

70 mil Measured Results

- 1 layer worked well, but as the layers increased, the expected gain enhancement was not present (max=10dBi)

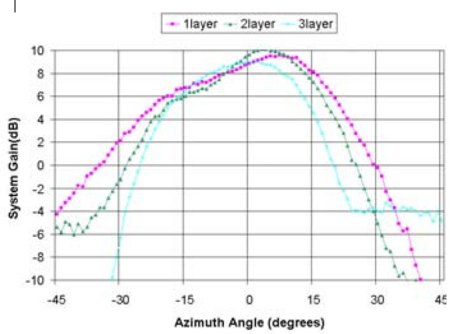

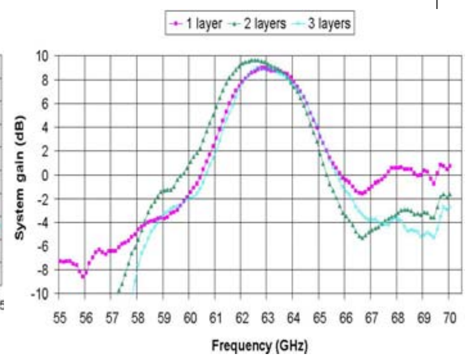

68 mil measured results

- Similar Result for 68 mil Structure
- Best System gain = 11.09 dBi

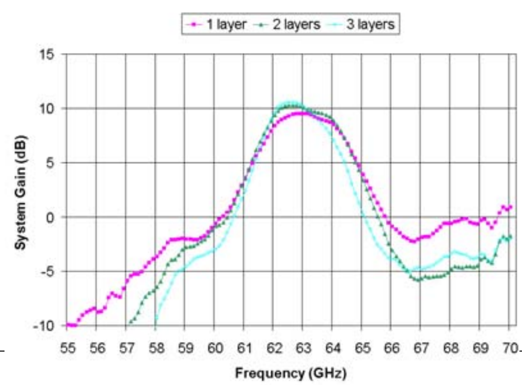

Thickness Variation

- Thickness was less than expected
- Thickness variation was greater than expected
- Grids became non-planar
- Multi-layer structures don't perform well, when all layers are not the same thickness

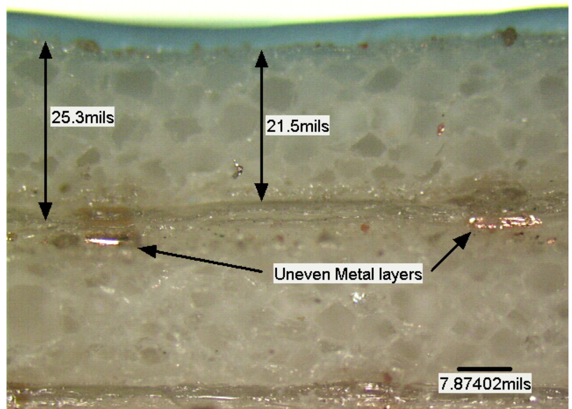

4 layer Thickness Measurement

- 1^{st} 3 layers averaged 38 mils, 4^{th} layer measured 35 mils
- All layers had at least 3 mil variations at edge
- This does not even include the curvature effect

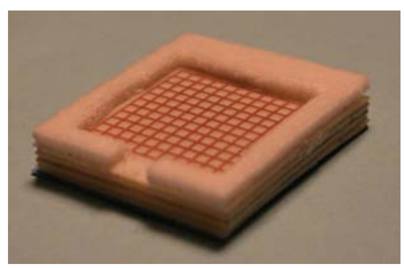

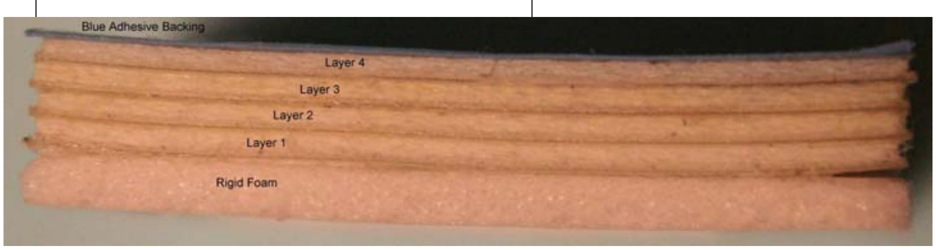

60GHz WLAN Experiments

1.25Gb/s – Pattern Triggered

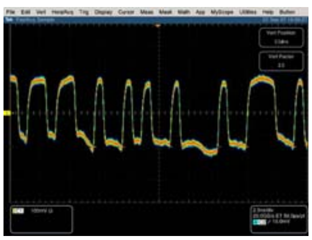

1.25 Gb/s – Eye Diagram

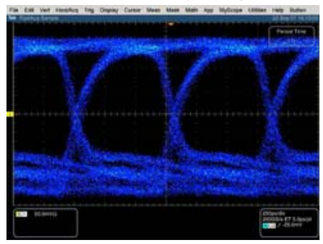

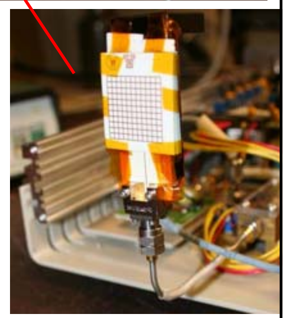

Actual 1.25 Gigabit/s Ethernet data was transmitted wirelessly between two computers using this high gain antenna structure

System gain = 11.09 dBi

Why the interest in electrically small antennas (ESAs)?

- Wireless technologies have become ubiquitous
- ESAs are one of their enabling technologies

$\lambda/4$ monopole
L = 250mm
for 300MHz

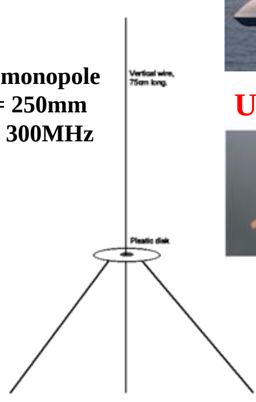

Typical antenna

UAVs

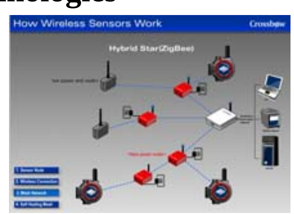

Wireless sensor networks

Embedded RFID tags

FOMs:
- Efficient
- High BW
- Multi-freq
- Low cost
- Light weight
- Easy fab

Efficient Electrically Small Antennas

Electrically small electric dipole = highly capacitive element

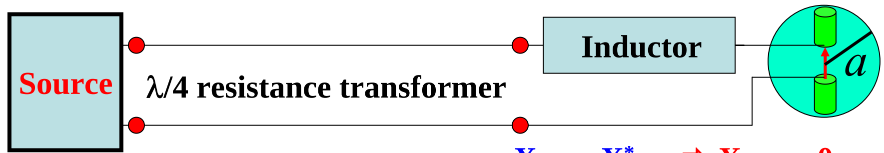

$X_{ind} = X^*_{ant}$ ⇨ $X_{total} = 0$

Input impedance matched to the source ⇨ $\Gamma = 0$
Max Accepted Power

Desire:

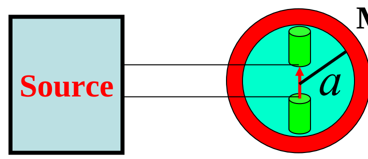

MTM "thing-a-ma-jigger"

- No matching circuit
- Efficient ESA

Center-fed dipole-ENG shell example: Using a highly subwavelength resonator to achieve a metamaterial-based *efficient* electrically-small antenna *(ESA)*

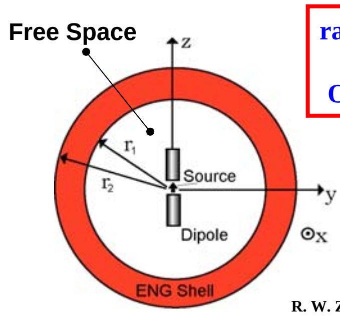

radius ~ λ/52
ka ~ 0.12
OE ~ 100%

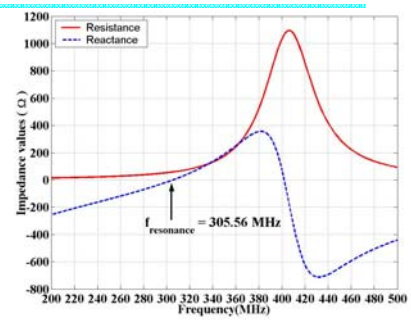

R. W. Ziolkowski and A. Erentok, IEEE Trans. Antennas Propagat., vol. 54, pp. 2113-2130, July 2006

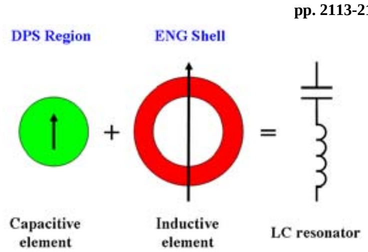

E-plane
and
H-plane
patterns

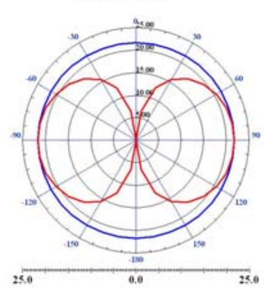

DARPA Sponsored, Boeing Phantom Works led project
PI: Minas Tanielian

Electrically Small Hemispherical Antenna

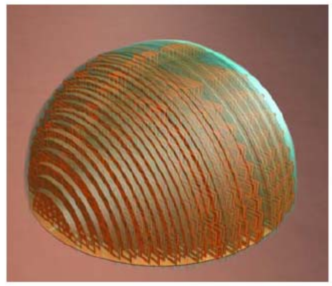

Many thanks to Bob Greegor for his program review slides

2nd Lower Loss MNG - 3mm x 3mm x 1mm Unit Cell

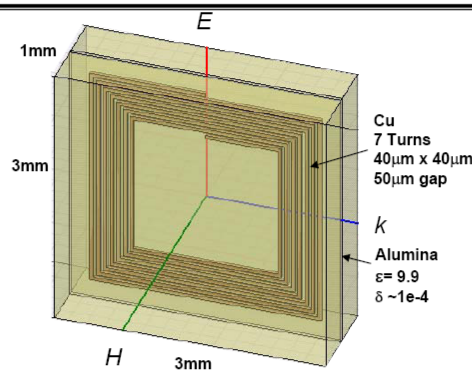

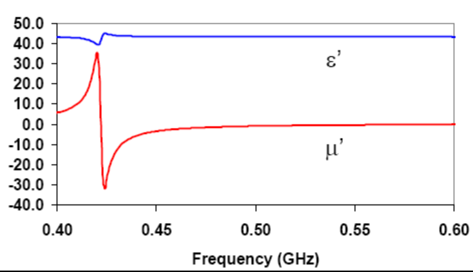

‘Amorphous’ Arrangement of Unit Cells

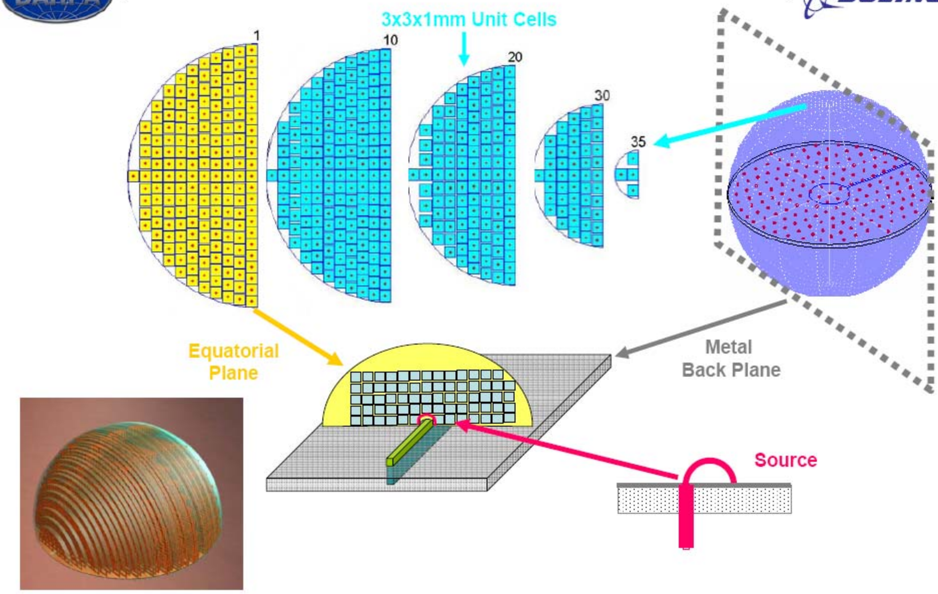

‘Crystalline’ Arrangement of Unit Cells

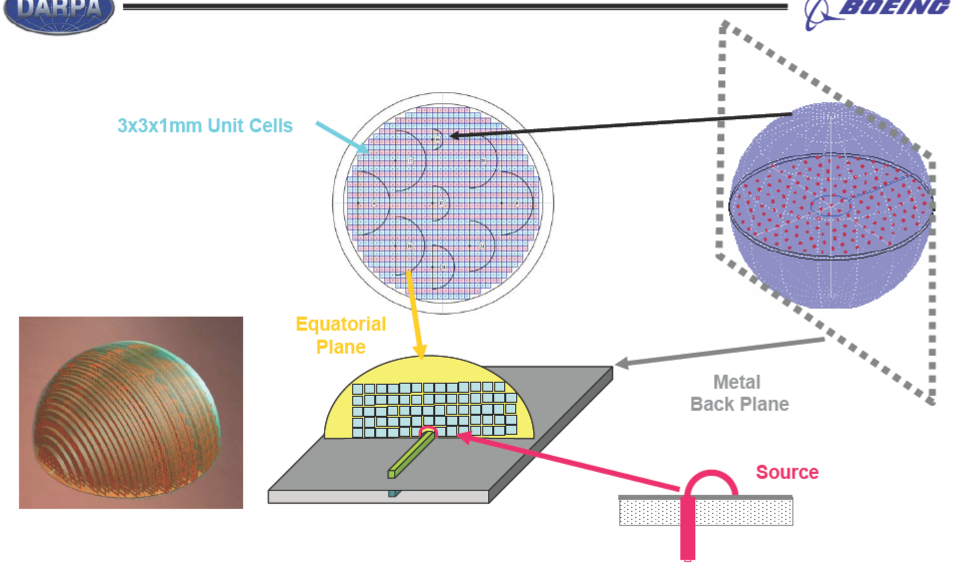

Assembled Hemispherical Antenna

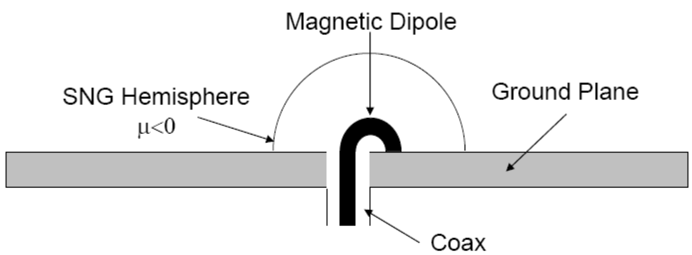

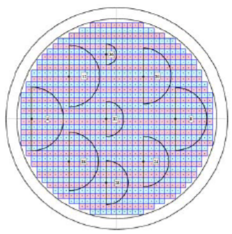

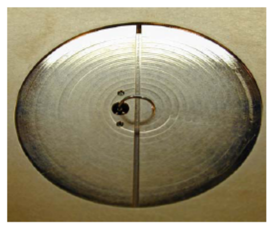

Assembled Hemispherical Antenna in Reverberation Test Chamber

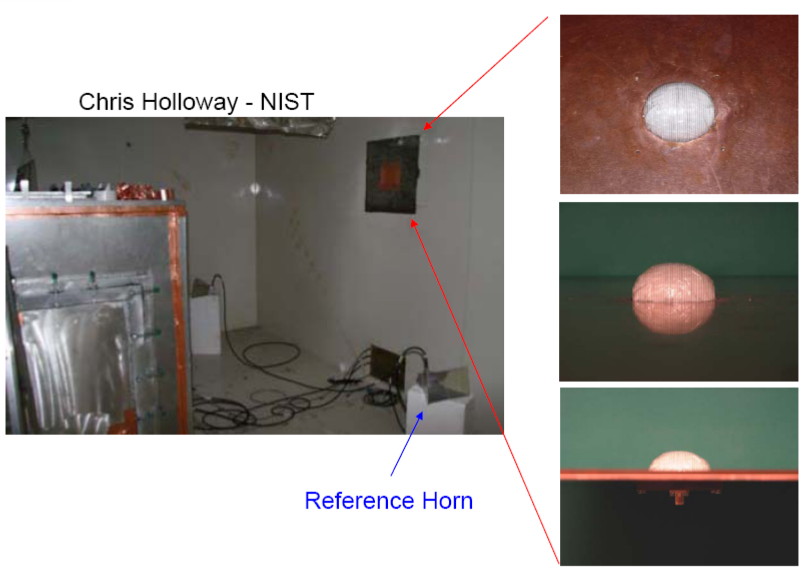

Radiated Power Relative to Horn for 3 Versions of Antenna

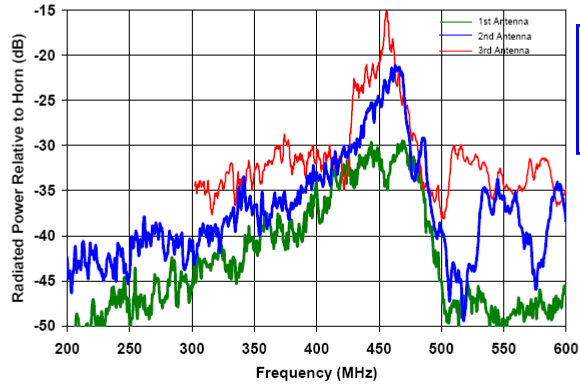

~17dB improvement over bare loop

1^{st} ANTENNA : Higher loss spiral unit cell on quartz, amorphous arrangement, R_L=5.0cm, R_S=3.5cm

2^{nd} ANTENNA: Lower loss sprial unit cell on alumina, crystalline arrangement, R_L=5.0cm, R_S=1.8cm

3^{rd} ANTENNA: Lower loss sprial unit cell on alumina, crystalline arrangement, R_L=9.0cm, R_S=1.8cm

Possible ENG shell meander-line realization

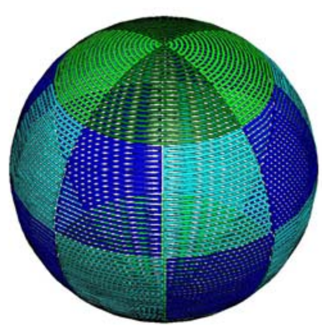

We have successfully developed several *metamaterial-inspired* efficient electrically-small antennas

EZ Magnetic | **EZ Electric**

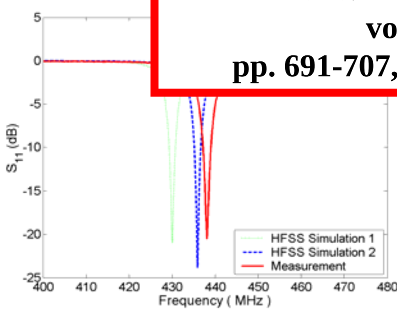

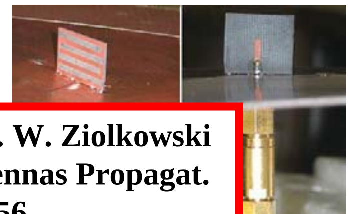

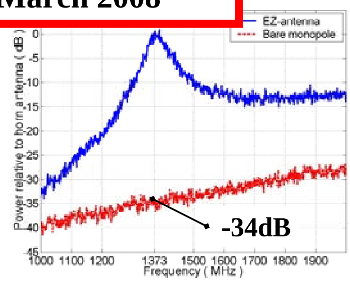

A. Erentok and R. W. Ziolkowski
IEEE Trans. Antennas Propagat.
vol. 56
pp. 691-707, March 2008

Optical Metamaterials and Applications Based on Resonant Coated Nano-Particles (CNPs)

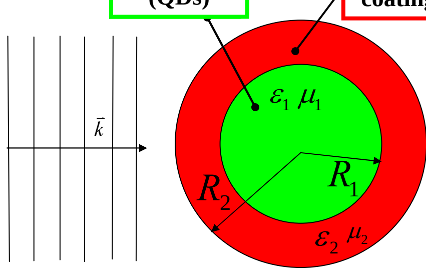

Excited by 500nm visible light
10nm, 30nm radius CNPs

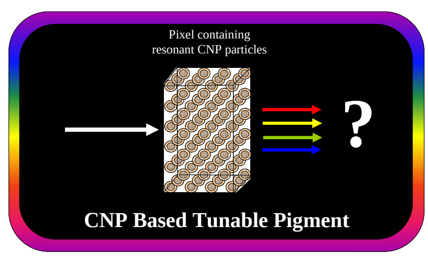

Three CNP layers generates the entire NTSC and RGB Gamuts

CNP Laser

Gain overcomes MTM Losses

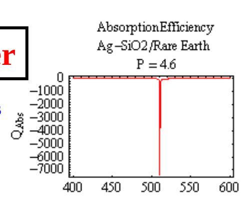

CNP Laser-based
Localized Nano-Sensors:
Bio, Chem -markers

Active Optical Metamaterials:
Overcome loss issues

J. A. Gordon and R. W. Ziolkowski
Opt. Exp., Vol. 15, Issue 5, pp. 2622-2653, March 2007

Metamaterials (MTMs) have exotic properties
that may have a high impact on a wide variety of practical applications

ENG
($\varepsilon < 0$, $\mu > 0$)

DPS
($\varepsilon > 0$, $\mu > 0$)

μ

UA Unit Cell
Lumped element
~ λ / 100

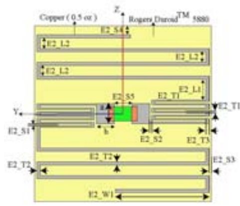

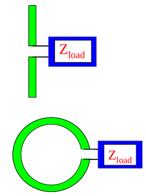

UA
Electric and Magnetic
Molecules
for
RAMs

Zero-index

ε

DNG
($\varepsilon < 0$, $\mu < 0$)

MNG
($\varepsilon > 0$, $\mu < 0$)

$n_{real} = -3.11$

loss = 0.91 dB/*cm*
at 400 MHz
for 10mm,
λ /75 unit cell

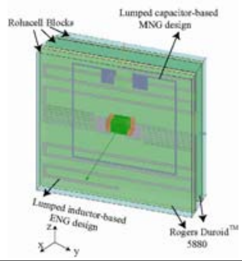

UA CLL AMC at X-band

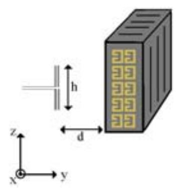

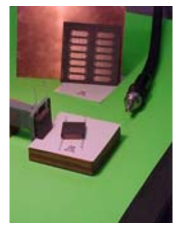

Thank you for listening ☺

Any questions ??